iScience

CellPress
OPEN ACCESS

Review

Silk-based wearable devices for health monitoring and medical treatment

Yu Song,[1,2,4,5,6] Chuting Hu,[1,2,4,5,6] Zheng Wang,[2,3,4,5,*] and Lin Wang[1,2,4,5,*]

SUMMARY

Previous works have focused on enhancing the tensile properties, mechanical flexibility, biocompatibility, and biodegradability of wearable devices for real-time and continuous health management. Silk proteins, including silk fibroin (SF) and sericin, show great advantages in wearable devices due to their natural biodegradability, excellent biocompatibility, and low fabrication cost. Moreover, these silk proteins possess great potential for functionalization and are being explored as promising candidates for multi-functional wearable devices with sensory capabilities and therapeutic purposes. This review introduces current advancements in silk-based constituents used in the assembly of wearable sensors and adhesives for detecting essential physiological indicators, including metabolites in body fluids, body temperature, electrocardiogram (ECG), electromyogram (EMG), pulse, and respiration. SF and sericin play vital roles in addressing issues related to discomfort reduction, signal fidelity improvement, as well as facilitating medical treatment. These developments signify a transition from hospital-centered healthcare toward individual-centered health monitoring and on-demand therapeutic interventions.

INTRODUCTION

After the COVID-19 pandemic, there has been a significant shift in personal health behavior. There is now an increased emphasis on annual physical examinations and physiological monitoring to identify diseases at an early stage and then enable timely intervention. This approach not only reduces costs but also improves clinical therapeutic outcomes. The physiological status of human body can be assessed through a set of highly correlated quantitative indexes such as heart rate, body temperature, biochemical metabolites, and biomarkers. Monitoring these physiological parameters allows for proper assessment of disease risk. Traditionally, health information is collected through invasive methods involving multiple blood samples. However, frequent blood tests are inconvenient for individuals requiring continuous monitoring over extended periods of time.[1] Moreover, conventional medical examinations like blood analysis, electrocardiogram (ECG), and electromyogram (EMG) are accurate but time-consuming and require professional technicians as well as substantial investments in equipment purchase and maintenance. Furthermore, regular hospital visits impose a heavy burden on healthcare resources and costs due to global population aging.[2] Therefore, there is a strong need for a more affordable and convenient approach that enables personalized medical monitoring.

Wearable sensors with multiple sensory functions[3,4] and even therapeutic effects[5,6] are considered to be an effective approach for health assessment, enabling personalized long-term healthcare, disease diagnosis, and prevention through clothes weaving or skin adhesion. These biosensors have the potential to significantly improve the quality of life for many patients, particularly those with chronic conditions. However, the rigidity, poor stretchability, and low resolution of commercial sensors manufactured using metal and semiconductor materials have limited their further application in wearable devices.[7,8] In recent years, flexible wearable sensors have emerged as a promising solution due to their excellent qualities of flexibility, comfort and noninvasive measurement capabilities.[9] By integrating wireless system into these sensors, the collected data becomes more accessible.[10]

Generally speaking, flexible wearable sensors consist of two main components: flexible substrates that ensure seamless biotic-abiotic interfaces with the skin; and functional components responsible for detecting and transmitting biochemical signals.[11] Currently used materials such as silicone rubber,[12] polyimide,[13] polydimethylsiloxane (PDMS),[14] and polytetrafluoroethylene[15] play vital roles in fabricating flexible sensors due to their excellent stretchability and bending performance. However, most of these materials require complicated synthetic processes which can be costly. Additionally, issues like insufficient biodegradability and biocompatibility may lead to pathological problems such

[1]Department of Clinical Laboratory, Union Hospital, Tongji Medical College, Huazhong University of Science and Technology, Wuhan 430022, China
[2]Research Center for Tissue Engineering and Regenerative Medicine, Union Hospital, Tongji Medical College, Huazhong University of Science and Technology, Wuhan 430022, China
[3]Department of Gastrointestinal Surgery, Union Hospital, Tongji Medical College, Huazhong University of Science and Technology, Wuhan 430022, China
[4]Hubei Key Laboratory of Regenerative Medicine and Multi-disciplinary Translational Research, Union Hospital, Tongji Medical College, Huazhong University of Science and Technology, Wuhan 430022, China
[5]Hubei Provincial Engineering Research Center of Clinical Laboratory and Active Health Smart Equipment, Union Hospital, Tongji Medical College, Huazhong University of Science and Technology, Wuhan 430022, China
[6]These authors contributed equally.
*Correspondence: zhengwang@hust.edu.cn (Z.W.), lin_wang@hust.edu.cn (L.W.)
https://doi.org/10.1016/j.isci.2024.109604

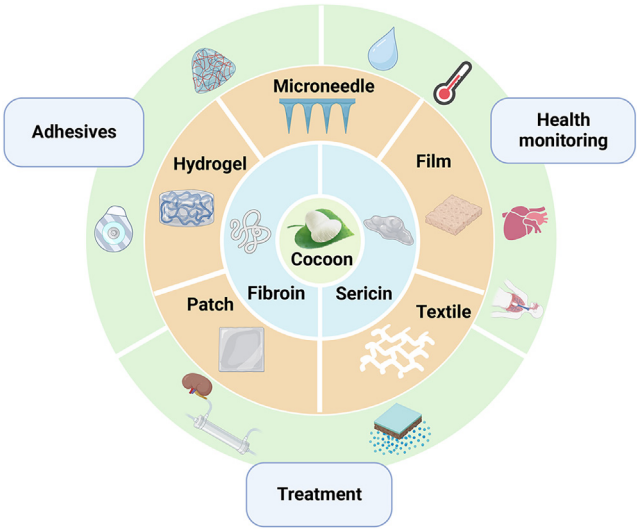

Figure 1. Different forms of silk-based wearable devices and adhesives in health monitoring and medical treatment

as skin rashes when attached on the skin for health monitoring purposes.[16] Therefore, it is crucial to design wearable sensors that are both user-friendly and compatible with human skin.

Due to its large-scale production, lightweight nature, and mechanical robustness, silk has been extensively developed in soft and breathable fabrics throughout history.[17] Nowadays, silk is considered as a highly promising material due to its two main components, silk fibroin (SF) and sericin. Both SF and sericin are functional, biodegradable, and biocompatible, and have been extensively applied in tissue engineering, regenerative medicine, and other biomedical fields.[18–21] Consequently, they are ideal choices for the constituents of wearable sensors.

Herein, we first introduce the remarkable intrinsic qualities of silk components. Subsequently, we summarize recent advancements in the study of silk-based wearable devices and adhesives for *in situ* monitoring or treatment purposes (Figure 1). Finally, we provide insights into further advancements that can be made with respect to silk-based wearable devices. It should be noted that this review will not cover silk-based strain/stress sensors as they have already been reviewed elsewhere.[22,23]

STRUCTURES AND PROPERTIES OF SILK PROTEINS

Silk is derived from the glands of spiders as well as certain insects such as silkworms, honeybees, and lacewings.[24] As a sustainable natural material that has been used in skin-friendly textile industry for centuries, silk, primarily extracted from *Bombyx mori* (*B. mori*) cocoons, has garnered significant attention in recent studies owing to its exceptional toughness (6×10^4–16×10^4 J/kg),[25] tensile strength (0.5–1.3 GPa),[26] tunable biodegradability,[27] and excellent biocompatibility.[27] Its enormous potential for application has been demonstrated across various domains including drug/gene delivery, tissue engineering, and soft electronics.[17,22,28]

The cocoon consists of double strands of SF forming the core of the silk fiber (70–80 wt %), which is surrounded by sericin (25–30 wt %).[29] SF is an FDA-approved natural biomaterial that has served as a suture material for centuries. The degumming procedures for separating SF from silk fibers include enzyme treatment, organic amines, pressurized steam, acid treatment, alkali treatment, soap solution, or water boiling.[30–35] After dissolution in solvents such as formic acid, trifluoroacetic acid, and lithium bromide,[36] SF can be processed into various formats (fibers, films, hydrogels, porous scaffolds) for diverse applications. SF is composed of light and heavy chains linked by disulfide bonds and stabilized by the glycoprotein P25 through noncovalent interactions.[37] The primary structure of heavy chains consists of hydrophilic non-repeating regions and hydrophobic repeating regions. The repetitive regions are predominantly comprised of Gly-X (GX) repeats. The $(Gly\text{-}Ala)_nGX$ (where X represents Ser or Tyr, and n represents the numbers of Gly-Ala repeats) blocks with different lengths and arrangements contribute to the formation of ordered secondary structures that play a major role in the mechanical properties of SF. For instance, highly repetitive Gly-Ala-Gly-Ala-Gly-Ser (GAGAGS) motifs generate anti-parallel β-sheet crystallites which confer excellent tensile strength and high toughness to SF. On the other hand, less repetitive Gly-Ala-Gly-Ala-Gly-Tyr (GAGAGY) motifs form semi-crystalline domains that produce type II β-turns, providing flexibility and elasticity to SF. In addition to β-sheet crystallites formation facilitated by van der Waals forces, hydrophobic interactions, and hydrogen bonds, other secondary structures including random coils and α-helices are also formed.[38] These additional structures have a negative impact on the mechanical strength of SF materials. In contrast, the light chains have non-repeating sequences including Ala (14%), Ser (10%), and Gly (9%), which form amorphous matrix and possess elasticity.[21] Unlike SF derived from mulberry silkworm (*Bombycidae* family), non-mulberry SF derived from *Saturniidae* family exhibits higher crystallinity due to the repetitive $(AA)_n$ and $(GG)_n$ blocks, resulting in superior mechanical properties.[18]

The versatile characteristics of SF, including ease of processing, adjustable water solubility, and high mechanical robustness, have been extensively investigated in wound healing,[22] drug delivery,[39,40] soft-tissue repair,[19] and wearable devices construction. SF can be endowed

with tunable conductivity through the introduction of graphene oxide (GO),[41] carbon nanotube (CNT),[42] and MXene.[43] Its functional groups (e.g., carboxyl, amidogen, hydroxyl, tyrosyl, and sulfhydryl) provide possibilities for biomolecules immobilization and functionalization.[44,45] The hydrophilic/hydrophobic properties, enzyme/drug release ratios, and degradation rates of SF are adjustable after thermal treatments.[23] Specifically, the increased degradation rate of SF could be programmed by lowering the proportion of β- sheet crystallites through the introduction of water molecules.[46,47] Meanwhile, procedures such as ethanol (or methanol) and water vapor treatments are suggested to increase the β-sheet content, achieving a slower degradation rate of SF.[36,48]

In contrast, sericin has long been discarded as a waste product during silk degumming process but is now recognized as a promising candidate in the biomedical field due to its superior properties of biocompatibility,[49] resistance to oxidation,[50] and ability to facilitate cell proliferation and adhesion.[51] Sericin (20–400 kDa) comprises 18 amino acids, with over half being polar amino acids such as lysine, aspartic acid, and serine. This contributes to the water-soluble nature of sericin.[52] Based on its water solubility, sericin can be divided into three layers from the outer to inner. The outer layer exhibits the highest water solubility.[53] Physical, chemical, and biological methods can all be used for extracting sericin. However, our previous study found that the mild LiBr extraction achieved a yield of 90% from fibroin-deficient mutant silkworms.[54] The secondary structures of sericin consist of random coils (63%) and β-sheets (35%), with no α-helix.[55] It has been suggested that β-sheets are positively associated with the firm structure of sericin. Furthermore, organic solvents like ethanol could increase their content in sericin.[56]

The properties, size, and morphology of sericin can be finely tuned through physical/chemical crosslinking, modification or precipitation, enabling its fabrication into various forms such as conduits, films, scaffolds, and hydrogels.[51] As a natural adhesive that binds SF together, sericin possesses bioadhesive properties. In a previous study, we utilized the hydrolysis of disulfide bonds in sericin to increase its hydrophobicity and fabricate a self-hydrophobized adhesive for sealing wounded wet tissue.[57] Moreover, due to the abundant presence of hydroxyl groups, amino groups, and carboxyl groups on the side chains of its hydrophilic amino acids which provide opportunities for ionic coordination interactions and hydrogen bonding formation, sericin holds great promise as a stabilizer and a binder in wearable devices.[20,58] Sericin has been introduced into materials to improve their electrical properties because polar biomolecules are advantageous for charge transfer.[59–61] For instance, sericin modification promoted the CNTs dispersion in water, resulting in remarkable electrochemical activity, sensibility, and electromagnetic shielding performance,[42,62,63] which makes up the deficiency of impaired electrical conductivity of CNTs using chemical modifications such as polymer grafting,[64] plasma treatment,[65] and oxidation,[66] and avoids problems such as decreased thermal conductivity, shortened length, and deformed surface structure of CNTs.

SILK-BASED WEARABLE SENSORS FOR HEALTH MONITORING

Silk-based wearable sensors have the potential to be affixed or worn on individuals for monitoring various health indicators, such as molecules/analytes in body fluids, body temperature, ECG, EMG, pulse, and respiration (Table 1).

Silk-based wearable sensors for monitoring of molecules/analytes within body fluids

Human body fluids contain a wealth of information regarding physiological status. The measurement of analytes within body fluids using wearable sensors typically involves redox reactions. The measurable electrical signals are correlated with the concentration of analyte in the sample. Currently, silk-based wearable sensors for humoral biomarker monitoring primarily focus on sweat electrolytes (e.g., Na^+ and K^+), metabolites (e.g., glucose and lactate), and biomolecules (e.g., ascorbic acid [AA] and uric acid [UA]) (Figure 2).

Diabetes mellitus is a metabolic disease resulting from insulin resistance or deficiency that affects approximately 382 million people worldwide, with China alone accounting for 150 million cases.[104,105] For diabetic patients, long-term glycemic management is crucially important.[106] Currently, almost all of the wearable biosensors fabricated for glucose monitoring rely on the oxidation reactions of glucose oxidase (GOD).[107] Notably, solid SF-based material created an environment conducive to the long-term stabilization of bioactive enzymes including GOD.[108] Accordingly, Zhao et al. created a minimally invasive microneedle-based biosensor wherein the silk/D-sorbitol composite aided in maintaining GOD activity under physiological conditions (Figure 2A). After 5 weeks at 4°C, 25°C, or 37°C, the remaining GOD signals were found to be 97.7%, 91.3%, and 76.9% of their original signal strength, respectively. H_2O_2 generated from the enzymatic reaction triggered the current variation, which was correlated with the glucose concentration. However, this biosensor has not yet been tested on the human body.[67]

The application of silk-based wearable sensors has also been investigated for monitoring other blood biomarkers, such as alpha-fetoprotein (AFP) and carcinoembryonic antigen (CEA), through the use of a 3D printed polyvinyl acetate (PVA)-SF patch with microchannels incorporating photonic crystal (PC) microspheres[68] (Figure 2B). Additionally, conductive ink-coated silk yarns were handloom-woven to manufacture multiplexed electrochemical sensor for detecting blood glucose and hemoglobin via chronoamperometry and differential pulse voltammetry methods[69] (Figure 2C). However, these sensors will need to be combined with microneedles for blood collection in later applications to achieve less painful detection with lower infection risk.

To increase the contact area for biochemical reactions and ion/molecular diffusion, enzymes were immobilized in a 3D functional SF nanofibrils (SFNFs) scaffold to fabricate an enzymatic sweat biosensor in a study. Compared with SF, SFNFs possessed a higher surface area, which achieved more efficient enzyme immobilization. SFNFs and enzymes together formed a bioactive porous enzymatic nanofiber (PEN) membrane. Then the combination of a platinum nanoparticles (PtNPs)/graphene nanocomposite film and PEN membrane permitted the effective electron transportation between electrodes and enzymes, resulting in prolonged lifespan and an elevated stability (25 h for glucose and 23.6 h for lactate). Furthermore, the wireless transmission of generated signals was enabled at any time using a bluetooth-enabled mobile handset.[70]

Table 1. Current silk-based wearable sensors for health monitoring

Indicator	Materials	Form	Component of silk	Reference
Body fluids				
Glucose	silk/polyols/GOD/Pt/Au	microneedle	fibroin	Zhao et al.[67]
AFP/CEA	SF/PVA/PC	patch	fibroin	Chu et al.[68]
Glucose/hemoglobin	silk yarns/conductive ink/GOD	textile	silk	Choudhary et al.[69]
Glucose/lactate	SFNF/GOD/lactic oxidase/ PtNPs/graphene	film	fibroin	Liu et al.[70]
Glucose	SF/AuNPs/GOD	film	fibroin	Meng et al.[71]
Glucose	silk/AuNPs/GOD	film	silk	Promphet et al.[72]
Glucose	silk/graphene/GOD/Pt nanospheres	film	fibroin	Liang et al.[73]
K^+/Na^+/UA/AA/lactate/glucose	silk/GOD/lactic oxidase	patch	silk	He et al.[10]
pH	SF/prodigiosin	film	fibroin	Liu et al.[74]
pH	silk/filter paper	textile	silk	Xiao et al.[75]
pH/Na^+/glucose	SF/GOD/thermoplastic adhesive	textile	fibroin	Zhang et al.[76]
Temperature				
	XSBR/SSCNT	film	sericin	Lin et al.[3]
	SNF/CNT	patch	fibroin	Gogurla et al.[77]
	silk/CNT	textile	fibroin	Wu et al.[78]
	SF/CNT/glycerol	film	fibroin	Zhang et al.[76]
	SF/MXene	hydrogel	fibroin	Duan et al.[79]
	SNF/copper/PET	film	fibroin	Wang et al.[80]
	SF/rGO	film	fibroin	Cho et al.[81]
	SF/CNC/RTP	hydrogel	fibroin	Wang et al.[82]
	SF/PNIPAM/PC	hydrogel	fibroin	Zheng et al.[83]
	TCS	textile	silk	Wang etal.[84]
ECG and EMG				
ECG	SSCNT ink	textile	sericin	Liang et al.[42]
EMG	SF/$CaCl_2$/Au	film	fibroin	Chen et al.[85]
ECG	SF/PEDOT:PSS	film	fibroin	Li et al.[86]
ECG/EMG	SNF/CNT	patch	fibroin	Gogurla et al.[77]
ECG/EMG	sericin/rGO/super adsorption polymer/cotton yarns	textile	sericin	Zhao et al.[87]
Pulse and respiration				
Pulse	SF/MXene	film	fibroin	Chao et al.[43]
Pulse	SF/MXene	film	fibroin	Wang et al.[88]
Pulse/respiration	XSBR/SSCNT	film	sericin	Lin et al.[3]
Pulse	SF/CNC/RTP	hydrogel	fibroin	Wang et al.[82]
Pulse	silk/CNT	textile	silk	He et al.[89]
Pulse	silk/rGO/ZnO nanorod	textile	silk	Mao et al.[90]
Respiration	sericin/CNT/rGO/AgNPs/ polyurethane fibers	textile	sericin	Bi et al.[91]
Pulse/respiration	SF/PEDOT	fibers	fibroin	Xing et al.[92]
Pulse	silk	textile	silk	Wang et al.[93]
Pulse	silk georgette	textile	silk	Wang et al.[94]
Pulse/respiration	silk yarns/di-aldehyde cellulose nanocrystals/polypyrrole	textile	silk	Dong et al.[95]
Pulse/respiration	silk/polyaniline	textile	silk	Cai et al.[96]

(*Continued on next page*)

Table 1. *Continued*

Indicator	Materials	Form	Component of silk	Reference
Pulse/respiration	silk yarns/polyaniline/CNTs	textile	silk	Ouyang et al.[97]
Respiration	SSCNT ink	textile	sericin	Liang et al.[42]
Respiration	SF/MXene	hydrogel	fibroin	Duan et al.[79]
Respiration	SF/rGO	film	fibroin	Cho et al.[81]
Respiration	SF/rGO	film	fibroin	Jiang et al.[98]
Respiration	SF/CNT	textile	fibroin	Ma et al.[99]
Respiration	SF/AM/AA	hydrogel	fibroin	Zhao et al.[100]
Respiration	SF/Ag nanowires	film	fibroin	Wen et al.[101]
Respiration	SF/MXene/$CaCl_2$	textile	fibroin	Yue et al.[102]
Respiration	SF/TA/borax/PVA	hydrogel	fibroin	Zheng et al.[103]

AA, ascorbic acid; AFP, alpha-fetoprotein; AM, acrylamide; Au, gold; AuNPs, gold nanoparticles; CEA, carcinoembryonic antigen; CNC, cellulose nanocrystals; CNT, carbon nanotube; ECG, electrocardiogram; EMG, electromyogram; GOD, glucose oxidase; PC, photonic crystal; PEDOT:PSS, poly(3,4-ethylenedioxythiophene):polystyrenesulfonate; PET, polyethylene terephthalate; PNIPAM, poly-N-isopropylacrylamide; PtNPs, platinum nanoparticles; PVA, polyvinyl acetate; rGO, reduced graphene oxide; RTP, reversible thermochromic pigment; SF, silk fibroin; SFNF, silk fibroin nanofiber; SSCNT, silk sericin carbon nanotube; TA, tannic acid; TCS, thermochromic silk; UA, uric acid; XSBR, carboxylic styrene butadiene rubber; ZnO, Zincoxide.

Due to its catalytic performance and remarkable stability, artificial nanozyme has gradually found applications in various fields such as environmental protection, biosensing, and disease treatment.[109] Among them, gold nanoparticles have emerged as a standout choice, due to their high catalytic activity, easily optimized nature, and superior stability.[110] Meng et al. successfully modified the N-doped porous carbonized SF substrate with gold nanoparticles (SF/AuNPs) to develop an electrochemical sensor for monitoring sweat glucose.[71] By coating the working electrode with SF/AuNPs and GOD, the sensor exhibited instantaneous detection of glucose concentration, achieving a detection limit of 23 μM through the electrochemical measurement of H_2O_2 generated from GOD oxidation. Furthermore, in another study, carbonized AuNPs-deposited silk fabric was employed for sweat urea detection within a wide range of 0–100 mM. The integration of laser desorption/ionization mass spectrometry realized data collection, thereby offering valuable insights for diagnosis of kidney diseases.[72]

Graphene, known as a two-dimensional light material, exhibits remarkable flexibility, and excellent electrical and mechanical properties, making it an ideal candidate for the conductive component of sensor. Recently, research has demonstrated the synthesis of high-strength structural materials by combining SF with GO through hydrophobic-hydrophobic, polar-polar, and hydrogen bonding interactions.[111,112] Building upon this concept, a composite film consisting of graphene and SF (G/S) was developed for glucose monitoring (Figure 2D). Notably, the film exhibited distinct morphologies on its two sides. The bottom side contained graphene sheets that infiltrated the silk fiber network, resulting in high electrical conductivity, the top side consisted of pure silk fibers that arranged in a hierarchical structure. The spatial distribution of graphene within the film led to different resistivities between these layers, making the G/S film a perfect supercapacitor and electrochemical electrode without any additional conductive additives. This innovative sensor composed of G/S film, Pt nanospheres, and GOD displayed significantly enhanced sensitivity (150.8 μA mM^{-1} cm^{-2}) compared to other glucose sensors,[113–115] enabling detection at an ultralow concentration down to1 μM.[73]

A multiplex sweat electrochemical sensor was utilized to simultaneously analyze six sweat biomarkers (K^+, Na^+, UA, AA, lactate, and glucose) in a creative work (Figure 2E). He et al. induced transformation of silk fabric into highly conductive carbonized silk with a porous and hierarchical structure through thermal treatment. Carbonized silk was then used to create six non-interfering working electrodes which were integrated into a multiplex sweat electrochemical sensor. Finally, by incorporating a signal collection and transmission component, real-time wireless information transfer to a mobile phone during exercise was enabled.[10]

Sweat pH could provide additional diagnostic information for skin diseases, wound infection, cystic fibrosis, and dehydration.[68] Liu et al. developed a pH-responsive film for monitoring sweat pH by incorporating prodigiosin into SF hydrogel[74] (Figure 2F). Prodigiosin, derived from microbial secondary metabolites, is a natural pH indicator.[116] The film exhibits reddish-purple color when the pH is below 8 and changed to orange and yellow as the pH increased from 8 to 10. Due to the biocompatible and biodegradable characteristics of prodigiosin and SF, the film can be safely attached to human skin and demonstrates corresponding color changes in response to artificial sweat with different pH values.

Xiao et al. designed an affordable microfluidic silk thread/paper-based sweat sensor system (Figure 2G). Firstly, a sweat reservoir was created using two cotton pads for sweat sample collection. Then, a combined colorimetric sensor was formed by applying universal pH indicator and a mixture of lactate hydrogenase and its substrate onto filter papers. By connecting the sweat reservoir with the sensor using a double-side adhesive tape and silk threads, they constructed the sensing device. With capillary channels formed between twisted filaments of hydrophilic silk thread, sweat was transported from the sweat reservoir to the sensing part for simultaneous measurement of both pH (4.0–8.0) and lactate (0–25 mM) levels. After being sewn in a hydrophobic arm guard, this device successfully detected sweat's pH levels as well as lactate concentration through RGB colorimetric analysis during exercise experiments, which yielded

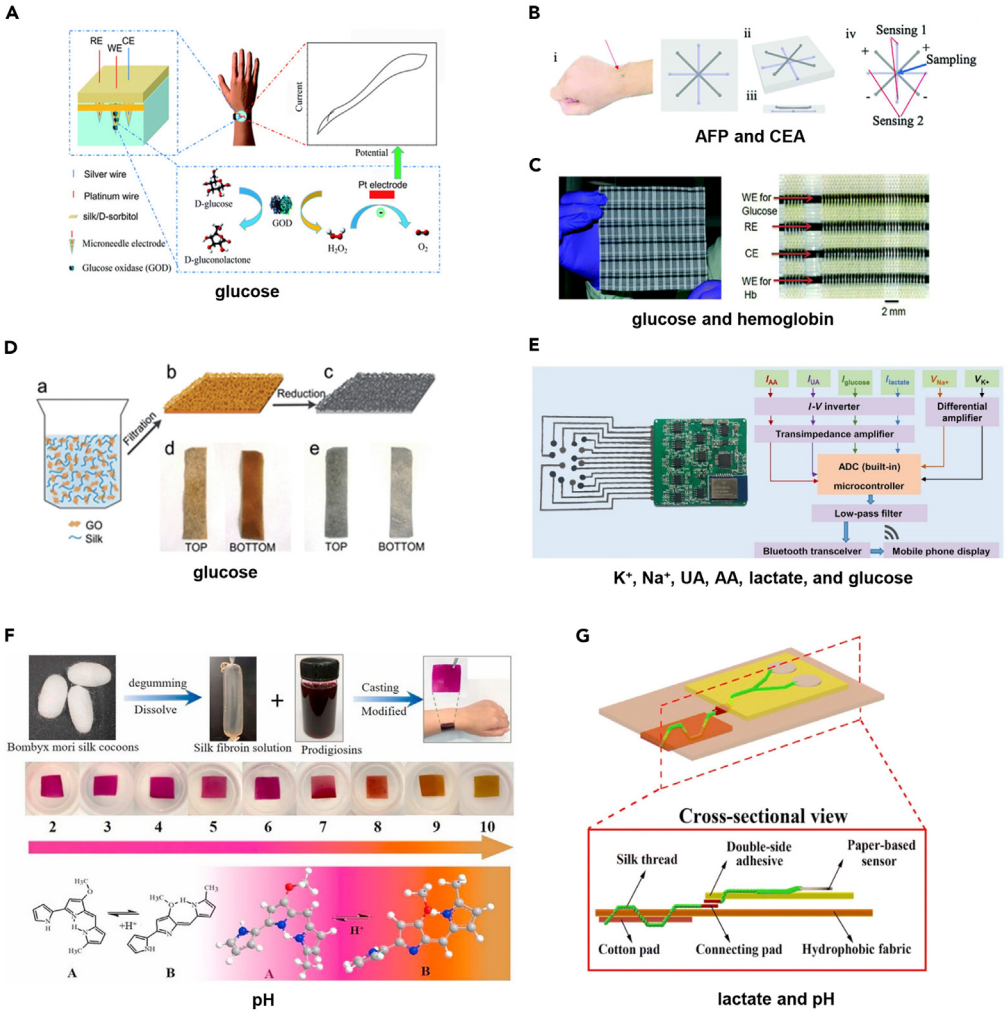

Figure 2. Silk-based wearable sensors for monitoring of molecule(s)/analytes within body fluids

(A) A silk/D-sorbitol microneedle-based biosensor was fabricated after integration with silver and platinum wires, the concentration of glucose was reflected by the variation of current changes. Reproduced with permission, from Zhao et al.,[67] Copyright 2020, Royal Society of Chemistry.

(B) A 3D printed PVA-SF patch sensor with microchannels was able to detect AFP and CEA. Reproduced with permission, from Chu et al.[68] Copyright 2021, Royal Society of Chemistry.

(C) Silk yarns were coated with conductive ink and then handloom-woven to present an electrochemical sensor for detection of glucose and hemoglobin. Reproduced with permission, from Choudhary et al.[69] Copyright 2015, Royal Society of Chemistry.

(D) G/S film with different morphology on both sides were used to build a sensor for glucose detection. Reproduced with permission, from Liang et al.[73] Copyright 2014, RSC Pub.

(E) A multiplex sweat electrochemical sweat sensor was fabricated on carbonized silk, the sensor achieved the simultaneous measurement of K^+, Na^+, UA, AA, lactate, and glucose and wireless transmission of data to mobile phones. Reproduced with permission, from He et al.[10] Copyright 2019, AAAS.

(F) A prodigiosin-contained SF film monitors sweat pH through color change. Reproduced with permission, from Liu et al.[74] Copyright 2022, Elsevier.

(G) A microfluidic silk thread/paper-based sweat sensor which was composed of a sweat reservoir and sensing parts was used for measuring sweat lactate and pH. Reproduced with permission, from Xiao et al.[75] Copyright 2020, Springer Nature.

comparable results with those obtained using a conventional pH meter or commercial lactate assay kit. However, it should be noted that variations in sweat's acidity may affect accurate detection of lactate levels. Hence, the results needed to be normalized with pH values of the same samples.[75] Zhang et al. also prepared a sweat sensor comprising of a sweat collection component and a detection module.[76] By introducing hydrophobic and hydrophilic modifications on opposite sides of carbonized SF, they ensured the directional transport of sweat. The sensor was finally assembled by bonding electrodes to modified SF fabric using thermoplastic adhesive. When attached to the skin, the sensor demonstrated capability in detecting pH levels, as well as concentrations of Na^+ and glucose within sweat.[76]

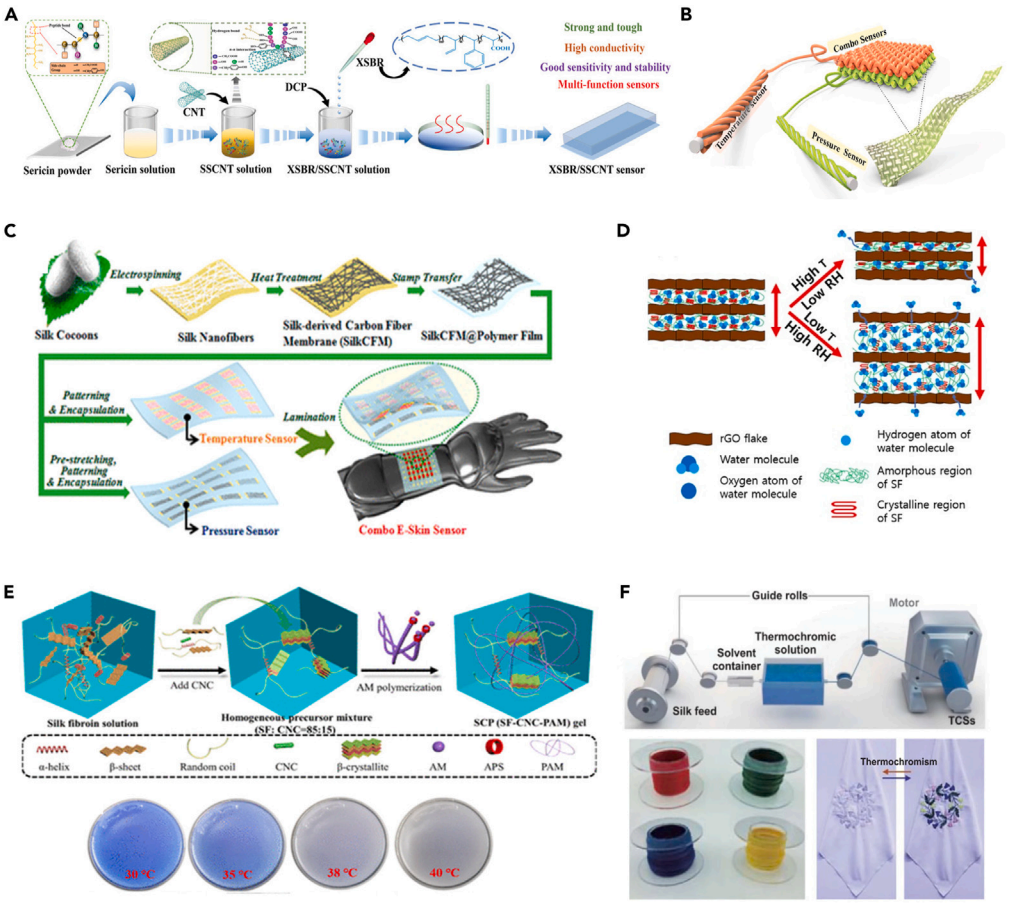

Figure 3. Silk-based sensors for monitoring of body temperature

(A) An XSBR/SSCNT film was used as temperature sensor due to its significant mechanical properties, electrical conductance and sensitivity. Reproduced with permission, from Lin et al.[3] Copyright 2021, John Wiley and Sons.

(B) Smart fabric made of fibrous sensors for temperature sensing. Reproduced with permission, from Wu et al.[78] Copyright 2019, John Wiley and Sons.

(C) A copper foil deposited with electrospun SNFs was carbonized to fabricate a temperature sensor, arrays of sensors on a PET film realized the spatial precision of sensing. Reproduced with permission, from Wang et al.[80] Copyright 2017, American Chemical Society.

(D) The temperature changes affected the water content within an SF/rGO film sensor, thus realizing temperature monitoring. Reproduced with permission, from Cho et al.[81] Copyright 2023, American Chemical Society.

(E) The SF/CNC/RTP gel showed a tough elastic interlocked network, taking advantage of thermochromism, the sensor became colorless from light blue as temperature rose within 30°C–40°C. Reproduced with permission, from Wang et al.[82] Copyright 2021, American Chemical Society.

(F) TCSs made from silk and thermochromic ink were used to fabricate smart fabrics for temperature sensing. Reproduced with permission, from Wang et al.[84] Copyright 2021, Springer Nature.

Silk-based sensors for monitoring of body temperature

Maintaining stable body temperature within the range of 36°C–37°C is crucial for human health as abnormal fluctuations can signify impairment in the central neural network's control over thermoregulation. This disruption can lead to various diseases or even mortality due to disrupted biochemical processes. Hence, the monitoring of body temperature is of vital importance (Figure 3).

CNTs have emerged as an exceptional conductive material for wearable temperature sensors owing to their superior thermal/electrical conductivity, chemical stability, and distinctive structural features that enable high photo/electro-thermal conversion efficiency. Lin et al. proposed a film of carboxylic styrene butadiene rubber (XSBR) modified with sericin and contained CNTs (XSBR/SSCNT)[3] (Figure 3A). The sericin modification prevented the inhomogeneous dispersion of CNTs in the polymer matrix, which was caused by strong π-π interactions and massive van der Waals forces.[62] As a result, the XSBR/SSCNT sensor exhibited significantly enhanced mechanical properties and electrical conductance,[3] enabling continuous monitoring of skin temperature within the physiological range with an impressive temperature coefficient of resistance (TCR) of 0.01636°C^{-1}. In another study, CNTs were dispersed into a porous silk nanofiber network (CNT/SNF) to create an ultrathin electronic tattoo (E-tattoo), exhibiting a low TCR of 5.2 × 10^{-3}°C^{-1}. The E-tattoo's resistance changes were used to infer body temperature based on its temperature-conductivity relationship.[77] Furthermore, fibrous sensors were fabricated by filling the gaps between silk fibers-sheathed polyester yarns with a mixture of CNTs and ionic liquid[78] (Figure 3B). The smart fabrics composed of these fibrous sensors

utilized the electrical insulating and thermal conductive properties of silk to achieve precise temperature sensing with a position precision of 1mm^2 and a TCR of 0.0123°C^{-1}. In addition, the encapsulation of dielectric elastomer provided protection against water immersion and machine washing. Furthermore, glycerol was introduced into the SF/CNT system to enhance flexibility. Exploiting the thermal effect of CNTs, elevated temperatures promoted electron transfer within and between CNTs, thereby augmenting conductance. Therefore, the SF/CNT/glycerol film achieved a sensitive monitoring of temperature from 25°C to 70°C with a TCR of 0.01644°C^{-1}.[76]

MXene, a two-dimensional transition metal carbide/nitride, exhibits metallic negative thermal coefficient behavior. Taking advantage of this property, Duan et al. fabricated an E-skin hydrogel by combining SF, MXene, $CaCl_2$, and H^+. Within the temperature range of 36°C–40°C, which corresponds to the human body temperature, the hydrogel showed nearly linear response characteristics, making it a suitable candidate for temperature sensing.[79]

The carbonization process of SF improved its electrical conductivity,[25] making it highly promising for wearable sensor applications.[29,117] A copper foil deposited with electrospun SNFs was thermally treated to obtain a carbon nanofiber membrane sensor with electrically conductive property. By placing an array of sensors on a polyethylene terephthalate (PET) film substrate, both on-skin temperature observation and spatial distribution of temperature within the range of 35°C–80°C were achieved[80] (Figure 3C).

The reduced graphene oxide (rGO) is a biocompatible derivative of GO with high electrical conductivity, making it an ideal candidate for sensing applications.[118] Using a layer-by-layer dip-coating fabrication method and thermal reduction treatment, a self-assembled SF/rGO film with a nacre-like structure was developed[81] (Figure 3D). A strong hierarchical interaction between SF and rGO contributed to the excellent mechanical properties of the film sensor. As rGO exhibits negative thermal expansion,[119] an increase in temperature led to the desorption of water molecules from the laminated layers of sensor, thereby enhancing the electrical contact between rGO flakes and enabling variations in electrical parameters to reflect changes in temperature.

Additionally, thermochromism also provides a convenient approach for the rapid and intuitive display of temperature through naked-eye color changes in temperature sensors. Wang et al. designed and constructed a self-healable gel based on SF and cellulose nanocrystals (SF/CNC) with *in situ* photopolymerization of acrylamide (Figure 3E). The CNC-induced reconstructed mesoscopic structure of SF contributed to the formation of a tough elastic network. With the addition of reversible thermochromic pigment (RTP), the color of SF/CNC gels quickly changed from dark blue to light blue, and finally became colorless within the 30°C–40°C temperature range.[82] PC is an artificial optical material that alters its structural color under external stimuli. And SF integration was reported to improve the mechanical properties of PC, thus opening up further applications in wearable sensors.[18] A study combined PC with dual-crosslinked hydrogel made from SF-poly-N-isopropylacrylamide (SF-PNIPAM) to present a blue nanocomposite film for body temperature detection. As the temperature reached 35°C, which is the critical phase transition temperature of SF-PNIPAM, hydrogen bonds within it were destroyed, leading to sudden shrinkage of SF-PNIPAM, destruction of PC close-packed structure, and the color change of nanocomposite film from blue to red.[83] What's more, without adding any thermochromic material, Wang et al. combined silk and thermochromic ink to create thermochromic silks (TCSs) via continuous dip-coating method and yarn spinning technique (Figure 3F). TCSs-based smart fabrics exhibited programmable and rapid thermochromic responses, demonstrating potential application of TCSs in wearable technology as well as temperature management.[84]

Silk-based wearable sensors for monitoring of ECG and EMG

Electrophysiological signals such as ECG and EMG are closely associated with cardiac and muscle health, with their characteristic waveforms obtained through direct electrodes-skin contact being well understood and interpretated. Abnormalities in these signals can serve as warning signs for heart diseases and neurologic impairment. Some silk-based sensors had also been designed for ECG and EMG measurement (Figure 4).

Liang et al. fabricated a textile ECG electrode using conductive SSCNT ink and integrated circuits (Figure 4A). The addition of sericin facilitated the homogeneous dispersion of CNTs by non-covalent contacts, leading to enhanced stability of the SSCNT ink. Subsequently, the electrode was fixed onto a compression shirt for ECG measurement, yielding high-fidelity ECG signals with intricate features.[42]

Chen et al. proposed a method for plasticizing SF into a stretchable film by introducing $CaCl_2$, which resulted in the transformation of stiff β-sheets of SF into extensible secondary structures such as random coils and helices, thereby improving the stretchability of SF. Then, a metal layer was deposited on the plasticized SF film to improve its conductivity. The low skin interfacial impedance endowed the film with outstanding electronic performance in EMG measurement, comparable to that of commercial gel electrodes without causing any discomfort[85] (Figure 4B).

Li et al. fabricated a thermal-wet comfortable ECG sensor by dip-coating SF fiber mats with conductive polymers poly(3,4-ethylenedioxythiophene): polystyrenesulfonate (PEDOT:PSS) (Figure 4C). In addition, the inclusion of glycerol in the coating solution improved the mechanical properties and stretchability of the silk mats. On the one hand, glycerol plasticization stabilized the fragile fiber mats by increasing stable β-sheet structures; on the other hand, it caused water retention in SF, which broke the hydrogen bonds in the amorphous domain of SF and increased the ratio of extensible secondary structures.[36] Moreover, glycerol facilitated the structural reorientation of PEDOT:PSS chains, enhancing both conductivity and stability of the coating.[120] Compared to commercial gel electrodes, silk-based electrodes exhibited comparable ECG signal acquisition with reduced noise peaks under sweaty conditions, which was ensured by their higher water-vapor transmission, lower evaporative resistance, lower thermal insulation properties, and greater stretchability.[86]

The aforementioned CNT/SNF patch demonstrated the capability to effectively monitor both ECG and EMG signals (Figure 4D). The recorded ECG signals exhibited clear PQRST waveforms, while the patch operated reliably even in hot and humid environments. What's more,

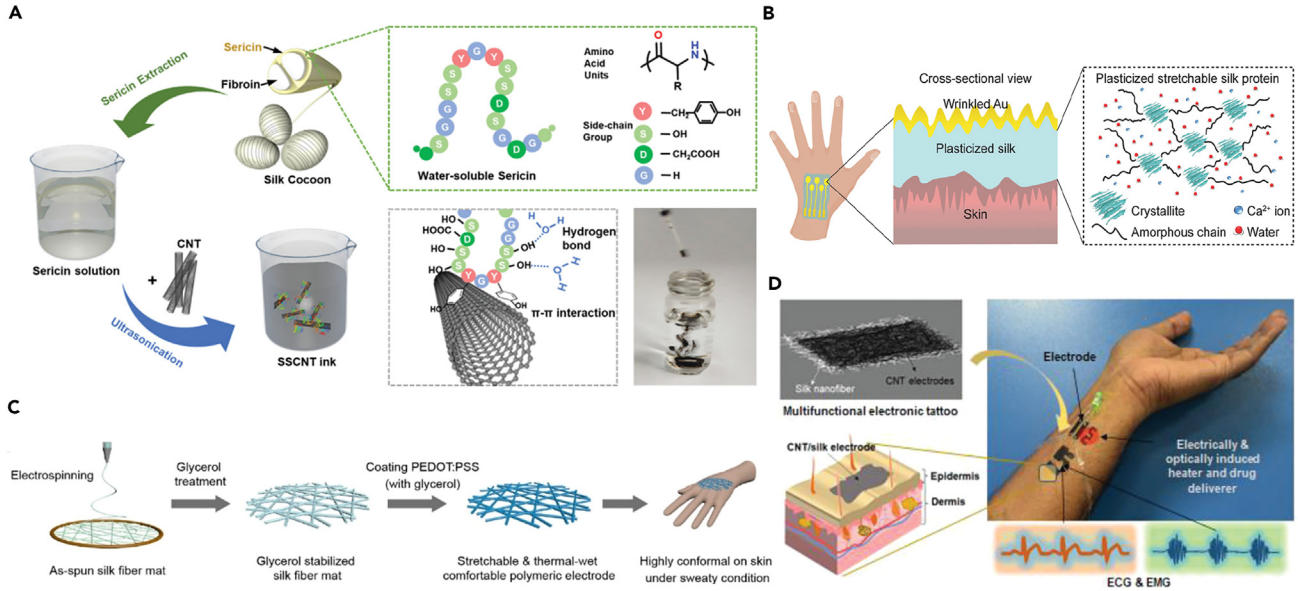

Figure 4. Silk-based wearable sensors for monitoring of ECG and EMG

(A) Sericin facilitated the homogeneous dispersion of CNT to form SSCNT ink, the SSCNT ink-based ECG electrode could be used for ECG signals collecting. Reproduced with permission, from Liang et al.[42] Copyright 2020, John Wiley and Sons.

(B) Ca^{2+} plasticization introduced water into SF film and increased its stretchability, together with a deposited metal layer, the electrode was presented for EMG measurement. Reproduced with permission, from Chen et al.[85] Copyright 2018, John Wiley and Sons.

(C) PEDOT:PSS-coated SF fiber mats were treated with glycerol to acquire a electrode for ECG monitoring under humid condition. Reproduced with permission, from Li et al.[86] Copyright 2021, American Chemical Society.

(D) a CNT/SNF E-tattoo attached to wrist skin for collecting ECG and EMG signals with details. Reproduced with permission, from Gogurla et al.[77] Copyright 2021, John Wiley and Sons.

the obtained ECG and EMG signals were comparable to those acquired using commercial conductive gels and gel electrodes, which typically require additional adhesive tapes or gels.[77]

Inspired by the art of embroidery, Zhao et al. successfully fabricated a 3D knitted electrode. They coated cotton yarns with conductive ink composed of rGO, sericin, and super adsorption polymers. Subsequently, the conductive yarns were woven into a textile electrode with a deep-textured and porous structure. In this design, sericin served as both a stabilizer of rGO through strong π-π interactions and a binder of cotton fibers. The incorporation of super adsorption polymer and the porous structure facilitated sweat absorption and release, dramatically improving the sensor performance under sweaty conditions. When integrated into clothing or attached to skin, the electrode enabled long-term capture of ECG signals with typical PQRST waveforms as well as EMG signals indicative of muscle fatigue during exercises.[87]

Silk-based sensors for monitoring of pulse and respiration

Pulse, a vital indicator of cardiac function, is synonymous with heart rate. Respiration is the process of gases exchange between the body and environment, ensuring adequate oxygen supply. The normal adult respiratory rate ranges from 12 to 20 breaths per minute, while pulse rate is four times higher. However, detecting the subtle vibrations caused by pulse and respiration remains challenging due to their intricate nature. Essentially, pulse sensors and breath sensors are both types of strain sensors with significantly higher sensitivity than those designed for human motion detection. Here, silk-based sensors for pulse and respiration convert tiny deformation signals into electrical signals primarily through piezoresistive effect (Figure 5).

MXene has gained significant attention for its outstanding electrical conductivity and hydrophilicity.[121] Hence, it was selected to fabricate a pressure sensor.[43] In DMSO solution, MXene sheets were mixed with tandem repeat proteins to prepare MXene ink. The electrode layer and the sensing layer of the pressure sensor were respectively printed and deposited on SF nanofiber membranes using MXene ink and MXene sheets. Enhanced loaded pressure induced an enlarged contact area between two layers, resulting in decreased resistance of pressure sensor. With a sensitivity as high as 298.4 kPa^{-1}, the pressure sensor can detect specific systolic peak (P1), diastolic peak (P2), and systolic upstroke time[43] that are related to arterial health and vascular aging[122] (Figure 5A). Additionally, acting as a bridging agent, SF promoted self-assembly of MXene nanosheets into a 3D wave-shaped composite film (Figure 5B). After sandwiching the film between Au/Cr electrodes and PET substrates, the pressure sensor was presented. Depending on changes in distance between adjacent MXene nanosheets and electrodes, the wrist pulse-induced force led to lower resistance of pressure sensor, thereby P1 and P2 pulse waveforms were clearly captured. Notably, SF endowed the sensor a higher sensitivity by lessening conductive channels between MXene sheets.[88] The multifunctional XSBR/SSCNT sensor mentioned in previous paragraph is also capable of monitoring pulse and respiration[3] (Figure 5C). When affixed to a wristband,

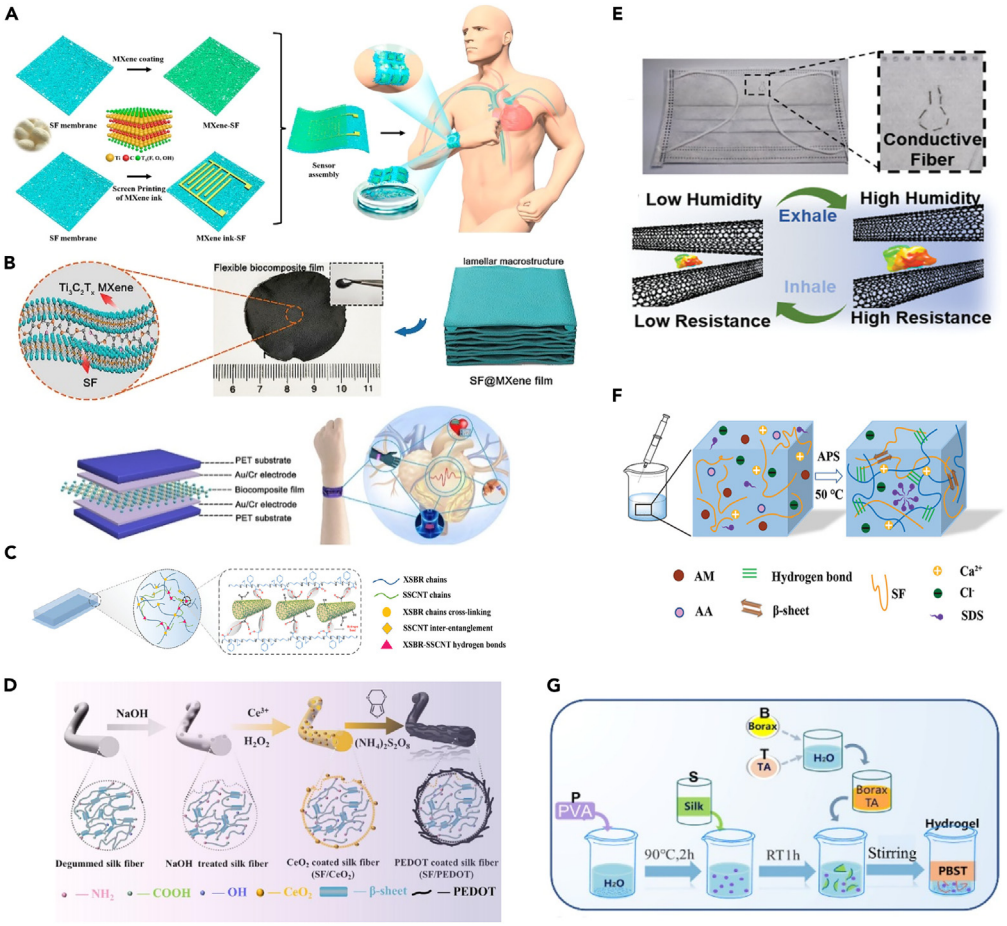

Figure 5. Silk-based sensors for monitoring of pulse and respiration

(A) MXene ink and MXene sheets were respectively printed and deposited on SF membrane to fabricate a MXene-SF film sensor for pulse detection. Reproduced with permission, from Chao et al.[43] Copyright 2021, American Chemical Society.

(B) SF contributed to the 3D cross-link structure of MXene-SF film by binding MXene sheets, the MXene-SF film was then assembled with PET substrates and Au/Cr electrodes to present a sensor for pulse monitoring. Reproduced with permission, from Wang et al.[88] Copyright 2020, Elsevier.

(C) An XSBR/SSCNT film sensor for pulse and respiration signals collection. Reproduced with permission, from Lin et al.[3] Copyright 2021, John Wiley and Sons.

(D) PEDOT was *in situ* chemically polymerized on conductive SF fibers to present an SF/PEDOT sensor for respiration and pulse monitoring. Reproduced with permission, from Xing et al.[92] Copyright 2023, Elsevier.

(E) A conductive SSCNT-coated fiber was sewn on a mask for respiration signals collection based on exhalation-induced humidity. Reproduced with permission, from Liang et al.[42] Copyright 2020, John Wiley and Sons.

(F) A composite SF/AM/AA hydrogel sensor for respiration measurement. Reproduced with permission, from Zhao et al.[100] Copyright 2021, John Wiley and Sons.

(G) The fabrication of a PBST hydrogel sensor for respiration detection. Reproduced with permission, from Zheng et al.[103] Copyright 2021, American Chemical Society.

the pulse waveforms display detailed information including diastolic wave (D-wave), tidal wave (T-wave), and percussion wave (P-wave). Moreover, when attached to clothing near the abdomen, different respiratory states such as deep breaths and shallow breaths can be accurately distinguished. With the establishment of a wireless-detection system, XSBR/SSCNT sensor could potentially be applied for continuous patient monitoring in intensive care units.[3]

In another study, the force generated by wrist pulse beating enhanced ionic movement inside an SF/CNC gel which led to changes in material resistance. However, only the intensity of pulse beating was inferred from irregular response waveforms with no further detailed information observed.[82] In contrast, XSBR/SSCNT sensor exhibited higher resolution. This might be attributed to its high sensitivity (gauge factor = 25.98), which resulted from the continuous conductive filler network formed by homogenous dispersion of SSCNT.

Relying on simple micro-dissolution of sericin on the surface of silk nonwoven fabric, CNTs were tightly adhered to silk nonwoven fabric, enabling the development of a sensitive wearable sensor. Based on the unique three-dimensional structure of silk fabric, this surface micro-dissolution and adhesion technology successfully improved the conductivity of the sensor. When attached to wrist, P1, P2, and dicrotic wave (P3) signals were precisely collected.[89] Applying a silk fabrics patch modified with rGO and ZnO nanorod on carotid artery also facilitated

pulse signals acquisition.[90] By combining sericin, CNTs, rGO along with antibacterial agent AgNPs, a conductive ink suitable for various substrates can be integrated with polyurethane fibers to manufacture respiratory sensing masks.[91]

Thanks to the abundant functional groups on silk, the *in situ* chemical polymerization of PEDOT on SF fibers enabled the fabrication of a strain sensor without reactions in solution and enhanced the reaction rate (Figure 5D). These conductive fibers possessed high electrical conductivity, enabling easy detection of slight strain signals generated from respiratory and pulse activities when sewn onto a mask or attached to the wrist. Specific details such as respiration depth and characteristic waveforms including P-wave, D-wave, and T-wave were accurately recorded.[92] Additionally, a carbonized silk fabric on a tight can also detect precise pulse signals.[93] Furthermore, with the help of medical adhesive tape, the carbonized silk georgette, a silk fabric made of strongly twisted warp and crepe weft, also successfully distinguished aforementioned pulse waveforms and different respiratory modes with a gauge factor of 173.0 for a strain of 60–100%.[94] Similarly, flexible textile sensors for both respiration and pulse monitoring were prepared using silk, di-aldehyde cellulose nanocrystals and polypyrrole through Schiff-base reaction.[95] Polyaniline, another conducting polymer with excellent electrochemical activity, was polymerized *in situ* on silk fabric by Cai et al. after pretreating with solvent ($CaCl_2/C_2H_5OH/H_2O$). This pretreatment increased the specific surface area of the sensor and led to a high loading of aniline monomers. By placing the sensor on wrist and chest, characteristic waveforms of human pulse and respiration modes were effectively collected.[96] Ouyang et al. prepared conductive paints using polyaniline and CNTs to modify silk yarns after applying the same solvent pretreatment ($CaCl_2/C_2H_5OH/H_2O$). The transformation induced by pulse and respiration increased the distance between conductive units and resistance in the sensor, enabling real-time health monitoring.[97] Instead of detecting changes in respiratory stress, Liang et al. selected exhaled humid gases as an indicator for the development of a respiration sensor (Figure 5E). A conductive yarn, printed with SSCNT hybrid ink, was sewn onto a mask. The presence of hydrophilic hydroxyl groups in sericin facilitated the expansion of the SSCNT network when water vapor from exhalation entered the air, thereby increasing the resistance of sensor. Conversely, inhaling reduced humidity levels in the air and consequently decreased sensor resistance. By monitoring these periodic alternations during inhaling and exhaling, abnormal breath patterns can be easily detected.[42] Similarly, expiratory moisture caused swelling of an SF/MXene/$CaCl_2$ hydrogel and increased interlayer spacing between MXene sheets, enabling the identification of respiratory patterns.[79] Since hydrophilic rGO is rich in oxygen-containing functional groups, humidity also interacted with the rGO flakes within the aforementioned SF/rGO sensor and another SF/rGO composites-based respiration sensor,[98] causing changes in their network structure and resulting in alterations of electrical conductance. Consequently, the rate of respiration was accurately detected,[81] Ma et al. developed hybrid fibers by combining regenerated SF with CNTs, which exhibited both conductivity and humidity-sensing ability. The changes in humidity affected conductivity of CNTs and cyclic contraction of SF, ultimately influencing the overall conductivity of the hybrid fibers. By embedding SF-CNT hybrid fibers into a facial mask, signals related to humidity-responsive resistance could be wirelessly transmitted for remote monitoring and diagnosis.[99] Additionally, a self-healing hydrogel composed of thermal polymerization of SF, acrylamide (AM), and acrylic acid (AA) was able to record respiratory rate and intensity through detecting heat from expiration at the same time (Figure 5F). SF was the core component of the hydrogel and optimized its mechanical property. The ion movement was accelerated with rising temperature, improving the conductivity of hydrogel. Hence, a hard breathing pattern exhibited bigger resistance changes.[100] Utilizing spray coating technology, Wen et al. employed Ag nanowires solution to coat electrospun SF films for the fabrication of an all-fiber sensor. The sensor exhibited excellent flexibility and air permeability due to SF serving as both the substrate and sensing component. Respiration-related humidity elevated the dielectric constant of SF, resulting in enhanced capacitance of the sensor.[101] Another example of hygroscopic materials is calcium-modified MXene/SF, where the introduction of calcium into the MXene/SF fibers promoted water absorption and provided additional ion migration pathways, enabling the detection of respiration at various frequencies on a mask-attached sensor.[102]

Zheng et al., fabricated a conductive hydrogel using a specific proportion of PVA, borax, SF, and tannic acid (TA), named PBST, which functioned as a respiratory sensor by detecting regular abdominal movement (Figure 5G). This hydrogel consisted of SF, TA, borax, and PVA in specific proportions.[103] In the dynamically cross-linked hydrogel network, SF played a crucial role in stabilizing the non-Newtonian behavior between borax and PVA by introducing energy dissipation mechanisms, thus elevating the viscoelasticity and self-healing properties of PBST. Additionally, SF formed cross-links with TA, an antibacterial component that facilitated the formation of highly adhesive hydrogel materials while minimizing its dissociation from the hydrogel network.[123] Subsequently, PBST was attached to a belt for respiration depth detection.

SILK-BASED ADHESIVE FOR HEALTH MONITORING

To ensure stable and precise collection of physiological parameters, establishing conformal and reliable contact between wearable devices and rough human skin is an indispensable precondition.[124] However, due to inadequate adhesion,[125] some epidermal sensors still require the assistance of double-sided medical tapes,[3] and the removal of these tapes can cause sharp pain. Moreover, their adhesion energy significantly decreases after repeated use.[126] In addition, during heavy exercise or physical work that causes sweating and mechanical deformations, conformal contact between skin and devices may be disrupted, hindering precision monitoring.[127] More importantly, preventing skin irritation and damage at the sensing site remains a challenge to be addressed, especially for people with wounded or fragile skin.[128] Therefore, there is a pressing need to develop a moisture-resistant adhesive that exhibits good biocompatibility and high signal-to-noise ratio.

Some methods have been proposed to address these issues. One approach involves chemical modification of the contact surface using materials such as aluminum, titanium elastomer, silicon, or glass.[129] However, residual chemicals can be harmful and cause skin irritation and itchiness. Another method involves applying fluorine-bearing ionogels which possess inherent hydrophobic networks providing anti-hydration ability. The low polarizability and strong electronegativity of fluorine contribute to low surface energy in fluorine-bearing polymers and therefore facilitating wet adhesion. But they still face challenges regarding biocompatibility.[130,131] Biocompatible materials including silica

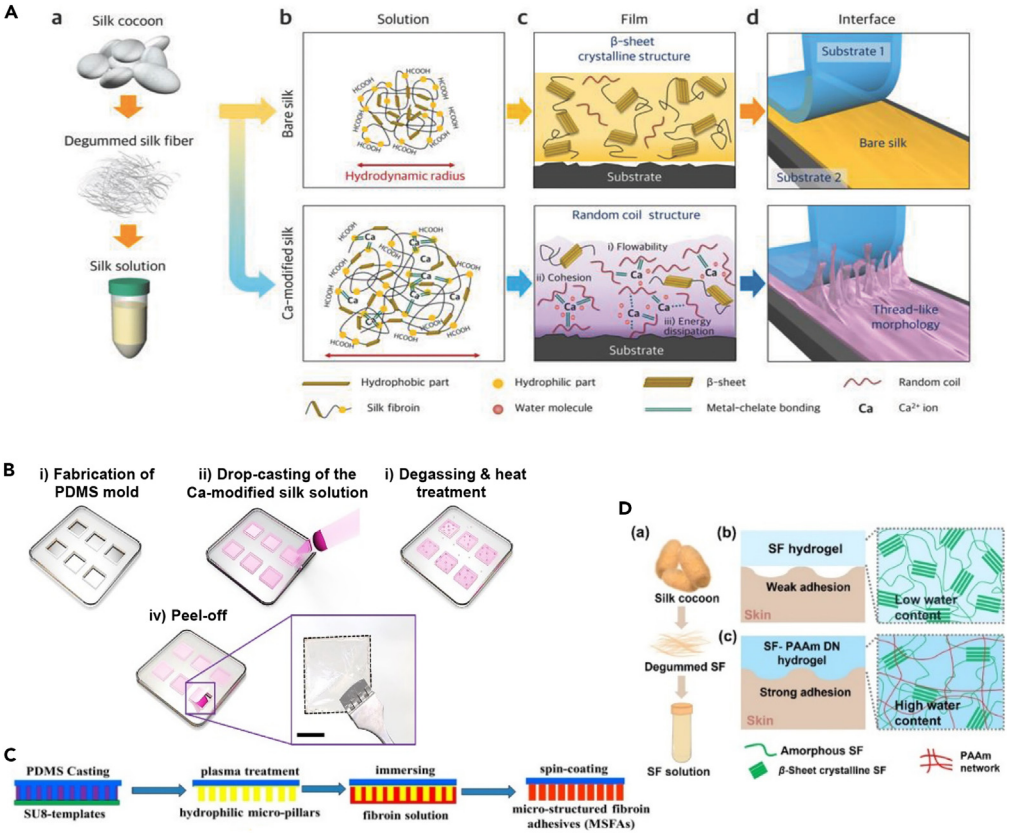

Figure 6. Silk-based adhesive for health monitoring

(A) The calcium-modification introduced more random coil structures into SF adhesive thus increasing mechanical interlocking and viscoelastic properties. Reproduced with permission, from Seo et al.[138] Copyright 2018, John Wiley and Sons.

(B) A calcium-modified SF adhesive was prepared in a PDMS mold. Scale bar: 1 cm. Reproduced with permission, from Lee et al.[139] Copyright 2021, American Chemical Society.

(C) An adhesive with unique micropillar structure enabled signals with high signal-to-noise ratio. Reproduced with permission, from Liu et al.[126] Copyright 2020, American Chemical Society.

(D) SF solution was prepared and the introduction of PAAm elevated the water content within SF adhesive and thereby improved its adhesive ability. Reproduced with permission, from Wang et al.[140] Copyright 2022, American Chemical Society.

nanoparticles solution,[132] poly(vinyl alcohol)-based gel,[133] and modified PDMS elastomer[134] have been considered as alternatives in order to eliminate dermal toxicity concerns, but they did not offer sufficient peel strengths required for protecting wearable devices from delamination.

As a natural protein with excellent biocompatibility and biodegradability, SF has been reported to exhibit strong adhesion to the epidermis through hydrogen bonds formed by its diverse amino acid residues.[135] SF-based bioadhesives have demonstrated resistance to wet conditions and potential for clinical applications[136] as well as tissue healing[137] (Figure 6). Specifically, calcium-modified SF has been developed as a reusable and non-allergenic adhesive for epidermal electronics[138] (Figure 6A). The incorporation of calcium ions increased the mechanical interlocking and viscoelastic properties of SF, significantly improving stretchability and tunable adhesion characteristics of the adhesive. Moreover, metal chelation of calcium ions provided appropriate cohesion and high energy dissipation, resulting in increased peel strength of SF adhesive and enabling effective transmission of strain signals to epidermal sensor systems. As a proof-of-concept demonstration, this adhesive ensures secure attachment of drug-loaded hydrogels onto the skin for subsequent transdermal drug delivery. Moreover, water molecules captured by calcium ions endowed the adhesive with electrical conductivity, enabling more stable ECG signal recordings with a lower noise level compared to commercial electrodes combined with either 3M adhesive or commercial hydrogel.[138] A wearable ultrasound patch consisting of calcium-modified SF showed low ultrasound transmission loss due to its acoustic impedance similarity to human skin. This patch demonstrated comparable performance to commercial ultrasound gel and held promising potential in various applications such as transcranial ultrasound neuromodulation, ultrasound heating, and ultrasound imaging[139] (Figure 6B).

The development of a micro-structured fibroin adhesive (MSFA) was undertaken to facilitate accurate acquisition of health information by epidermal devices. MSFA demonstrated robust and adjustable adhesion with the skin under humid conditions. Unlike medical tape, the unique micropillar structure of MSFA mitigated sharp pain associated with high peeling force. Subsequently, integration of MSFA with a pulse sensor enabled clear visualization of crucial parameters such as tricuspid valve opening, dicrotic notch, peak systolic pressure, and forward

wave in the output signals (Figure 6C). Signal-to-noise ratio serves as an indicator for assessing the relative effectiveness of signal transmission. Remarkably, incorporation of MSFA into the pulse sensor resulted in significantly higher signal-to-noise ratio compared to using a single sensor without MSFA, thereby enhancing epidermal signal transmission considerably. What's more, the exceptional durability and reusability characteristics of MSFA achieved long-term and stable monitoring for personal healthcare applications.[126]

Focusing on offering SF adhesive with adjustable adhesion to wet surfaces, a study aimed to reduce the content of β-sheet crystallites in SF adhesive by maintaining internal water content (Figure 6D). Polyacrylamide (PAAm), a hydrophilic and biocompatible high-molecular polymer, exhibits excellent water-absorbing qualities due to the hydrolytic reaction of its internal acylamino group into carboxylate radical.[141] Hence, the hydrophilic PAAm network was introduced into SF hydrogel to create an SF-PAAm hydrogel adhesive that exhibited superior adhesion compared to medical tape and commercial silicone gel (Mepoform). By integrating signal collection and transmission components, a wet-resistant sweat sensor capable of detecting pH levels as well as concentrations of Ca^{2+}, K^{+}, and Na^{+} in sweat was successfully fabricated.[140]

SILK-BASED WEARABLE DEVICES FOR MEDICAL TREATMENT

Silk-based wearable artificial kidney system

The kidney is a vital excretory organ in the human body, primarily functioning as a filtration system to maintain electrolyte balance through excreting metabolic waste and excess water.[142] Chronic kidney disease (CKD) occurs when an individual's glomerular filtration rate (GFR), the standard indicator of renal function, remains below 60 mL/min per 1.73 m^2 for more than 3 months. End stage renal disease (ESRD) represents the final and most severe stage of CKD progression, rendering the kidneys incapable of sustaining life.[103] Dialysis and kidney transplant are common treatment options for ESRD patients, with approximately 2.5 million individuals worldwide undergoing dialysis.[143] Dialysis can be categorized into hemodialysis or peritoneal dialysis modalities. Although hemodialysis is more commonly utilized, peritoneal dialysis offers unique advantages such as increased feasibility in remote and rural areas, lower nurse-to-patient ratios, and greater technical simplicity.[144]

In recent years, the development of the wearable artificial kidney (WAK) system has aimed to achieve enhanced efficiency and convenience in continuous dialysis. Within a circular WAK system, the dialysate solution is continuously regenerated and reused to effectively eliminate uremic toxins from the body[145] (Figure 7). Urea, being a predominant component among these toxins, consistently exhibits a strong correlation with poor prognosis.[147] Despite recent proposals of various strategies, satisfactory results have not yet been achieved due to significant toxic side effects[148] and limited adsorption capacity.[149] To address these issues, researchers immobilized urease onto SF membranes to fabricate noncytotoxic urea filters with high solute removal efficiency, adequate biocompatibility, and cost-effectiveness for use in WAK systems[145,146] (Figure 7). Urea was catalyzed by the immobilized urease to produce carbon dioxide and ammonia. The hydrophilicity of SF significantly enhanced the water-binding abilities of the filtration system, resulting in improved urea removal efficiency. Moreover, due to strong binding between SF membrane and urease, the filter could be reused up to 7 cycles with only slight decrease in enzyme activity. In tests using a 50 mg/dL urea solution, this filter achieved a 50% removal rate within 20 min and even reached 90% after filtering peritoneal dialysate for 24 h[146] (Figure 7A). In a subsequent experiment, authors integrated an upgraded version of this filter that included polymer-based spherical carbonaceous adsorbent (PSCA)[145] (Figure 7B). After treating patient dialysate with this new system for 24 h, it not only removed 99% of urea but also reduced 95% of other uremic toxins including phosphorus, uric acid, creatinine as well as 50% of β2-microglobulin. In addition, this filter system removed more toxins from blood serum than traditional dialysate exchange system when tested on uremia rat. These studies demonstrated great potential for practical application of SF membranes in peritoneal dialysate regeneration by acting as an enzyme-immobilization substrate which benefits toxins absorption in WAK systems.

Silk-based wearable devices for drug delivery

Recently, silk proteins have been widely explored for their application in incorporation of multiple functional materials (e.g., CNTs, laser dyes, and graphene) in forms of hydrogels, fibers, films, etc. In addition, studies reported that the intermolecular interaction between biomolecules and SF chains allowed for the preservation of bioactivity in labile biological components including antigens, antibodies, enzymes, and drugs over an extended period of time.[150–153] Consequently, these unique characteristics of silk proteins offer a superior alternative for further strategies in real-time drug delivery (Figure 8).

On the basis of high light-to-heat conversion efficiency of CNTs and the excellent heat conductivity property of SNF, a CNT/SNF patch was fabricated and applied to pig skin (Figure 8A). A fluorescent dye rhodamine B was used as a model drug loaded into SNF and successful penetration of rhodamine B was observed from cross-sectional images after light-induced heating. The study demonstrates the potential application of optically induced heating in wearable epidermal drug delivery platforms.[77]

Epilepsy is a chronic but severe neurological disorder affecting approximately 65 million individuals worldwide, with 20%–40% of this population at risk for body injury due to persistent seizures.[155] Given the unpredictability and perniciousness of a sudden seizure onset, continuous monitoring and immediate treatment are crucial. To enable real-time monitoring and *in situ* controllable treatment, a sensing patch composed of microneedle arrays assembled with an SF-CNT hydrogel containing thermo-activated papain was developed (Figure 8B). The entire patch was affixed to the back of nude mice to detect the epilepsy-induced body convulsions. The hydrogel served as a drug carrier and a strain sensor while the microneedles acted as conduits for drug delivery and filters to prevent CNTs from entering the mouse's body based on their size. Upon recording epileptic symptoms, laser heating was applied to induce temperature-sensitive papain-mediated degradation of hydrogel and subsequent drug release. Then, epileptic convulsions were alleviated after a 10-min light-triggered medical treatment. However, it should be noted that laser heating was artificially applied rather than directly

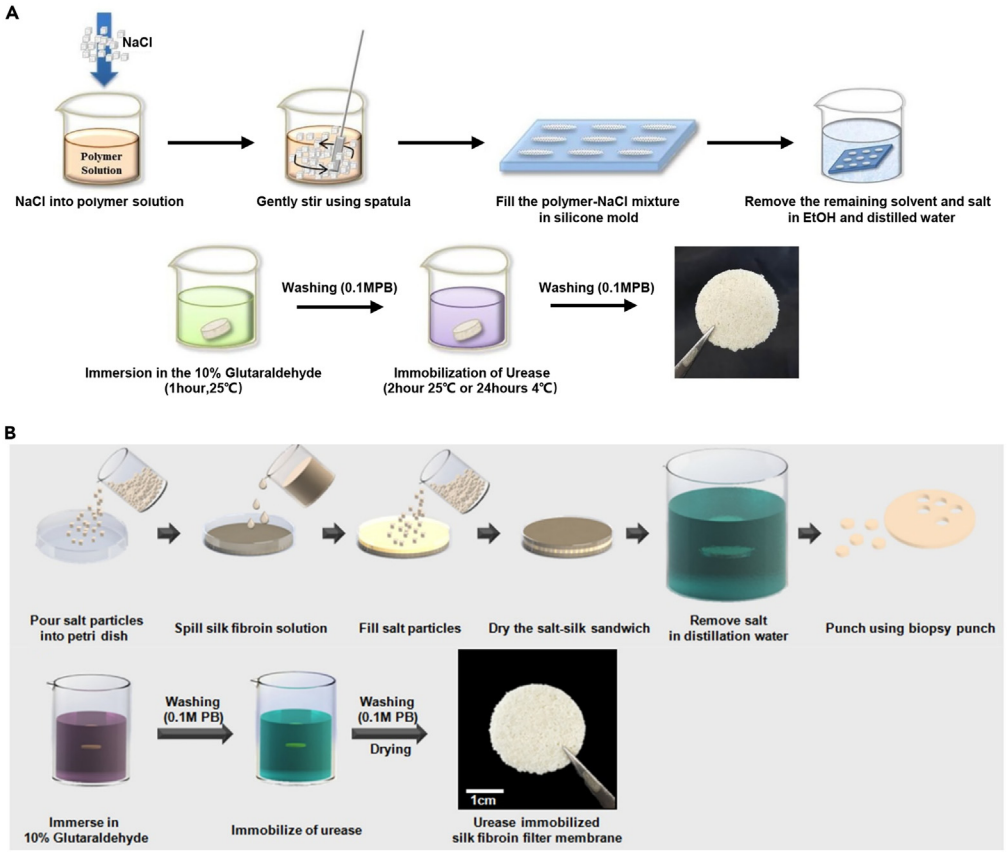

Figure 7. Silk-based wearable artificial kidney system

(A) A urease-immobilized SF membrane was fabricated for removing urea. Reproduced with permission, from Moon et al.,[146] Copyright 2016, John Wiley and Sons.
(B) A urease-immobilized SF membrane was fabricated for removing uremic toxins. Reproduced with permission, from Sultan et al.[145] Copyright 2019, Elsevier.

triggered by body convulsions, thus further optimization may be necessary regarding the linkage between body convulsions and heating treatment.[5]

To promote hindlimb regeneration in adult Xenopus laevis following amputation, a wearable bioreactor was developed using progesterone-containing silk hydrogel and a protective silicone rubber outer shell (Figure 8C). The device was attached to the amputation site of Xenopus laevis as an adjunctive therapy for successful delivery of progesterone. A series of regenerative activities were confirmed genetically and morphologically after 24 h of treatment.[154] Although direct application of the wearable bioreactor for human limb repair is not yet feasible, it holds potential for treating small-scale injuries.

CONCLUSION AND FUTURE PROSPECTIVES

By utilizing SF and sericin, wearable devices for sensory or therapeutic applications can be fabricated. In all the aforementioned studies, SF played a crucial role in device formation by serving as fundamental material scaffolds, immobilization matrices, or substrates. Meanwhile, sericin primarily acted as an adhesive or stabilizer. Through compatible contact with highly deformable tissues with or without the help of adhesive, silk-based wearable sensors are capable of obtaining a wide range of parameters including humoral indexes, temperature, ECG, EMG, pulse, and respiration. In some cases, they may even be used for disease treatment. Together, silk-based wearable devices provide an attractive alternative for household health management and are especially useful for people with chronic disease. They greatly increase the possibilities of identifying emergency events during intervals between periodical hospital visits and ultimately pave the way toward realizing transformation from traditional reactive episodic healthcare to predictive and proactive diagnostics.

Nevertheless, certain limitations still need to be addressed for further development. In order to achieve high conductivity in wearable sensors, the introduction of polymer conductors or metal electrodes has been explored. However, the low biodegradability and biocompatibility of these materials pose risks to both human health and the environment. Therefore, greater efforts should be devoted to exploring conductive materials that are not only biocompatible but also bioabsorbable, ensuring sustainable development of wearable sensors. Notably, carbonized SF[10,80] and SSCNT[3,42] have been reported as both conductive and biocompatible options for use in health monitoring.

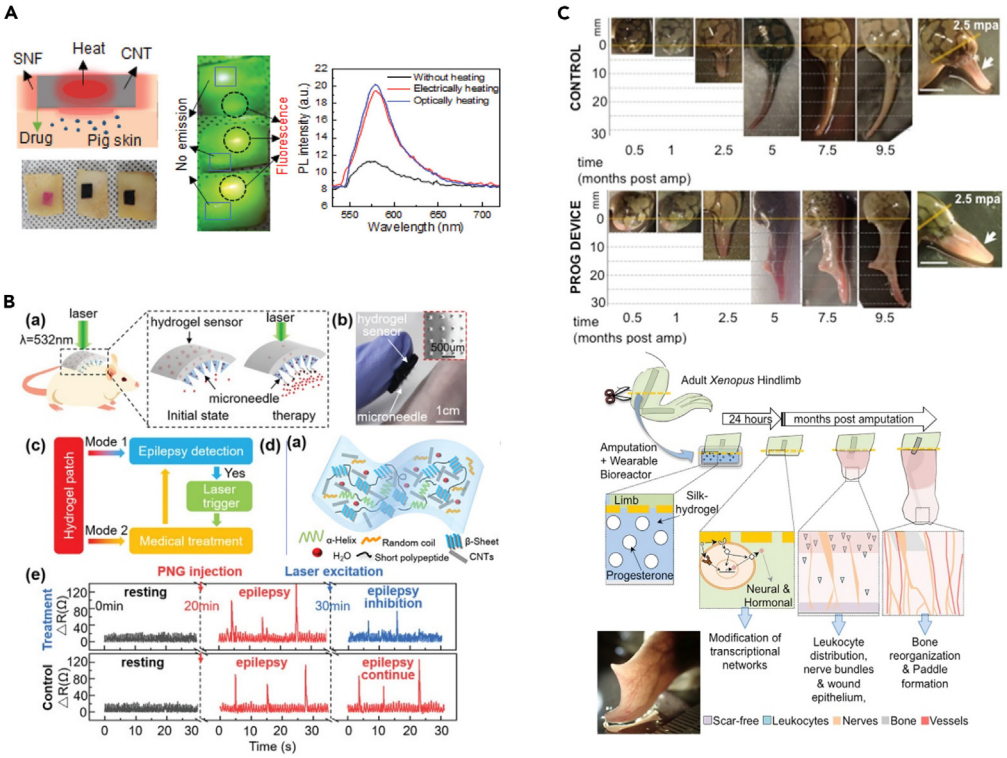

Figure 8. Silk-based wearable devices for drug delivery

(A) A CNT/SNF patch realized heat-stimulated drug delivery of rhodamine B (a model drug) on pig skin. Reproduced with permission, from Gogurla et al.[77] Copyright 2021, John Wiley and Sons.

(B) An SF-CNT hydrogel sensor integrated with microneedle arrays for laser-triggered drug delivery as an epilepsy treatment. Reproduced with permission, from Zhang et al.[5] Copyright 2020, John Wiley and Sons.

(C) A progesterone-containing silk hydrogel bioreactor was used for successful drug delivery in hindlimb regeneration of adult Xenopus laevis following amputation. Scale bar: 1 cm. Reproduced with permission, from Herrera-Rincon et al.[154] Copyright 2018, Elsevier.

As for the mechanical performance of wearable sensors, silk-based sensors with low water content exhibit high robustness but lack stretchability. While high robustness contributes to sensor durability, good stretchability is essential for optimal contact between skin and devices. Therefore, significant efforts should be made toward achieving a balance between robustness and stretchability in silk-based sensors or simultaneously improving both aspects. Furthermore, enhancing the mechanical characteristics of textile-based wearable sensors is crucial for achieving long lifespan. It has been observed that silk from wild *Antheraea pernyi* cocoons exhibited better mechanical performance compared to *B. mori* cocoons varieties, suggesting potential utility of different silkworm cocoons types for improved durability.[156]

Finally, the prevalence of wearable sensors derived from sericin is not as widespread as those from SF, potentially due to the hindered development resulting from long-term neglect in the silk industry and misconceptions regarding adverse biological responses caused by sericin. Researchers also need to address the challenge of achieving large-scale production of high-quality sericin protein without denaturation and degradation. Numerous unknowns await further exploration.

ACKNOWLEDGMENTS

This work was supported by the National Key Research and Development Program of China (2022YFC2408100), the National Natural Science Foundation of China Programs (81901904, 82072167, and 82272277).

AUTHOR CONTRIBUTIONS

Y.S.: Conceptualization, writing – review and editing. C.T.H.: Conceptualization, writing-original draft. Z.W. and L.W.: Supervision and fund acquisition. Y.S. and C.T.H. contributed equally to this work.

DECLARATION OF INTERESTS

The authors declare no competing interests.

REFERENCES

1. Harpak, N., Borberg, E., Raz, A., and Patolsky, F. (2022). The "bloodless" blood test: intradermal prick nanoelectronics for the blood extraction-free multiplex detection of protein biomarkers. ACS Nano *16*, 13800–13813. https://doi.org/10.1021/acsnano.2c01793.
2. Yang, Y., and Gao, W. (2019). Wearable and flexible electronics for continuous molecular monitoring. Chem. Soc. Rev. *48*, 1465–1491. https://doi.org/10.1039/c7cs00730b.
3. Lin, M., Zheng, Z., Yang, L., Luo, M., Fu, L., Lin, B., and Xu, C. (2022). A high-performance, sensitive, wearable multifunctional sensor based on rubber/CNT for human motion and skin temperature detection. Adv. Mater. *34*, 2107309. https://doi.org/10.1002/adma.202107309.
4. Li, P., Sun, Z., Wang, R., Gong, Y., Zhou, Y., Wang, Y., Liu, X., Zhou, X., Ouyang, J., Chen, M., et al. (2022). Flexible thermochromic fabrics enabling dynamic colored display. Front. Optoelectron. *15*, 40. https://doi.org/10.1007/s12200-022-00042-3.
5. Zhang, S., Zhou, Z., Zhong, J., Shi, Z., Mao, Y., and Tao, T.H. (2020). Body-integrated, enzyme-triggered degradable, silk-based mechanical sensors for customized health/fitness monitoring and in situ treatment. Adv. Sci. *7*, 1903802. https://doi.org/10.1002/advs.201903802.
6. Chen, M., Li, P., Wang, R., Xiang, Y., Huang, Z., Yu, Q., He, M., Liu, J., Wang, J., Su, M., et al. (2022). Multifunctional fiber-enabled intelligent health agents. Adv. Mater. *34*, 2200985. https://doi.org/10.1002/adma.202200985.
7. Zhou, J., Guo, X., Xu, Z., Wu, Q., Chen, J., Wu, J., Dai, Y., Qu, L., and Huang, Z. (2020). Highly sensitive and stretchable strain sensors based on serpentine-shaped composite films for flexible electronic skin applications. Compos. Sci. Technol. *197*, 108215. https://doi.org/10.1016/j.compscitech.2020.108215.
8. Qiu, A., Li, P., Yang, Z., Yao, Y., Lee, I., and Ma, J. (2019). A path beyond metal and silicon: polymer/nanomaterial composites for stretchable strain sensors. Adv. Funct. Mater. *29*, 1806306. https://doi.org/10.1002/adfm.201806306.
9. Liu, J., Liu, M., Bai, Y., Zhang, J., Liu, H., and Zhu, W. (2020). Recent progress in flexible wearable sensors for vital sign monitoring. Sensors *20*, 4009. https://doi.org/10.3390/s20144009.
10. He, W., Wang, C., Wang, H., Jian, M., Lu, W., Liang, X., Zhang, X., Yang, F., and Zhang, Y. (2019). Integrated textile sensor patch for real-time and multiplex sweat analysis. Sci. Adv. *5*, eaax0649. https://doi.org/10.1126/sciadv.aax0649.
11. Baeg, K.J., and Lee, J. (2020). Flexible electronic systems on plastic substrates and textiles for smart wearable technologies. Adv. Mater. Technol. *5*, 2000071. https://doi.org/10.1002/admt.202000071.
12. Jiang, Y., Wang, Y., Wu, H., Wang, Y., Zhang, R., Olin, H., and Yang, Y. (2019). Laser-etched stretchable graphene-polymer composite array for sensitive strain and viscosity sensors. Nano-Micro Lett. *11*, 99. https://doi.org/10.1007/s40820-019-0333-6.
13. Qin, Y., Peng, Q., Ding, Y., Lin, Z., Wang, C., Li, Y., Xu, F., Li, J., Yuan, Y., He, X., and Li, Y. (2015). Lightweight, superelastic, and mechanically flexible graphene/polyimide nanocomposite foam for strain sensor application. ACS Nano *9*, 8933–8941. https://doi.org/10.1021/acsnano.5b02781.
14. Chen, K., Luan, M., Xiong, H., Zhang, J., Zhang, J., Gao, G., Chen, P., Zhu, A., and Yu, C. (2018). Polydimethylsiloxane (PDMS)-based flexible resistive strain sensors for wearable applications. Appl. Sci. *18*, 345. https://doi.org/10.3390/app8030345.
15. Park, H., Lee, S., Jeong, S.H., Jung, U.H., Park, K., Lee, M.G., Kim, S., and Lee, J. (2018). Enhanced moisture-reactive hydrophilic-PTFE-based flexible humidity sensor for real-time monitoring. Sensors *18*, 921. https://doi.org/10.3390/s18030921.
16. Besio, W., Sharma, V., and Spaulding, J. (2010). The effects of concentric ring electrode electrical stimulation on rat skin. Ann. Biomed. Eng. *38*, 1111–1118. https://doi.org/10.1007/s10439-009-9891-y.
17. Huang, W., Ling, S., Li, C., Omenetto, F.G., and Kaplan, D.L. (2018). Silkworm silk-based materials and devices generated using bio-nanotechnology. Chem. Soc. Rev. *47*, 6486–6504. https://doi.org/10.1039/c8cs00187a.
18. Dang, X., Song, Z., and Zhao, H. (2020). Signal amplified photoelectrochemical assay based on Polypyrrole/g-C_3N_4/WO_3 inverse opal photonic crystals triple heterojunction assembled through sandwich-type recognition model. Sensor Actuat. B Chem. *310*, 127888. https://doi.org/10.1016/j.snb.2020.127888.
19. Gholipourmalekabadi, M., Sapru, S., Samadikuchaksaraei, A., Reis, R.L., Kaplan, D.L., and Kundu, S.C. (2020). Silk fibroin for skin injury repair: Where do things stand? Adv. Drug Deliv. Rev. *153*, 28–53. https://doi.org/10.1016/j.addr.2019.09.003.
20. Lamboni, L., Gauthier, M., Yang, G., and Wang, Q. (2015). Silk sericin: a versatile material for tissue engineering and drug delivery. Biotechnol. Adv. *33*, 1855–1867. https://doi.org/10.1016/j.biotechadv.2015.10.014.
21. Kundu, B., Rajkhowa, R., Kundu, S.C., and Wang, X. (2013). Silk fibroin biomaterials for tissue regenerations. Adv. Drug Deliv. Rev. *65*, 457–470. https://doi.org/10.1016/j.addr.2012.09.043.
22. Wang, C., Xia, K., Zhang, Y., and Kaplan, D.L. (2019). Silk-based advanced materials for soft electronics. Acc. Chem. Res. *52*, 2916–2927. https://doi.org/10.1021/acs.accounts.9b00333.
23. Sun, Q., Qian, B., Uto, K., Chen, J., Liu, X., and Minari, T. (2018). Functional biomaterials towards flexible electronics and sensors. Biosens. Bioelectron. *119*, 237–251. https://doi.org/10.1016/j.bios.2018.08.018.
24. Preda, R.C., Leisk, G., Omenetto, F., and Kaplan, D.L. (2013). Bioengineered silk proteins to control cell and tissue functions. Methods Mol. Biol. *996*, 19–41. https://doi.org/10.1007/978-1-62703-354-1_2.
25. Prakash, N.J., Mane, P.P., George, S.M., and Kandasubramanian, B. (2021). Silk fibroin as an immobilization matrix for sensing applications. ACS Biomater. Sci. Eng. *7*, 2015–2042. https://doi.org/10.1021/acsbiomaterials.1c00080.
26. Cebe, P., Hu, X., Kaplan, D.L., Zhuravlev, E., Wurm, A., Arbeiter, D., and Schick, C. (2013). Beating the heat - fast scanning melts silk beta sheet crystals. Sci. Rep. *3*, 1130. https://doi.org/10.1038/srep01130.
27. Pritchard, E.M., Valentin, T., Panilaitis, B., Omenetto, F., and Kaplan, D.L. (2013). Antibiotic-releasing silk biomaterials for infection prevention and treatment. Adv. Funct. Mater. *23*, 854–861. https://doi.org/10.1002/adfm.201201636.
28. Blake, S., Kim, N., Kong, N., Ouyang, J., and Tao, W. (2021). Silk's cancer applications as a biodegradable material. Mater. Today Sustain. *13*, 100069. https://doi.org/10.1016/j.mtsust.2021.100069.
29. Wen, D.L., Sun, D.H., Huang, P., Huang, W., Su, M., Wang, Y., Han, M.D., Kim, B., Brugger, J., Zhang, H.X., and Zhang, X.S. (2021). Recent progress in silk fibroin-based flexible electronics. Microsyst. Nanoeng. *7*, 35. https://doi.org/10.1038/s41378-021-00261-2.
30. Gulrajani, M.L. (1992). Degumming of silk. Rev. Prog. Coloration *22*, 79–89. https://doi.org/10.1111/j.1478-4408.1992.tb00091.x.
31. Luong, T.-H., Dang, T.-N.N., Ngoc, O.P.T., Dinh-Thuy, T.-H., Nguyen, T.-H., Van Toi, V., Duong, H.T., and Le Son, H. (2015). Investigation of the Silk Fiber Extraction Process from the Vietnam Natural *bombyx Mori* Silkworm Cocoon (Springer), pp. 325–328. https://doi.org/10.1007/978-3-319-11776-8_79.
32. Vyas, S.K., and Shukla, S.R. (2016). Comparative study of degumming of silk varieties by different techniques. J. Text. Inst. *107*, 191–199. https://doi.org/10.1080/00405000.2015.1020670.
33. Kusurkar, T.S., Tandon, I., Sethy, N.K., Bhargava, K., Sarkar, S., Singh, S.K., and Das, M. (2013). Fluorescent silk cocoon creating fluorescent diatom using a "water glass-fluorophore ferry". Sci. Rep. *3*, 3290–3298. https://doi.org/10.1038/srep03290.
34. Rastogi, S., and Kandasubramanian, B. (2020). Progressive trends in heavy metal ions and dyes adsorption using silk fibroin composites. Environ. Sci. Pollut. Res. Int. *27*, 210–237. https://doi.org/10.1007/s11356-019-07280-7.
35. Reizabal, A., Costa, C.M., Pérez-Álvarez, L., Vilas-Vilela, J.L., and Lanceros-Méndez, S. (2023). Silk fibroin as sustainable advanced material: material properties and characteristics, processing, and applications. Adv. Funct. Mater. *33*, 2210764. https://doi.org/10.1002/adfm.202210764.
36. Rockwood, D.N., Preda, R.C., Yücel, T., Wang, X., Lovett, M.L., and Kaplan, D.L. (2011). Materials fabrication from *Bombyx mori* silk fibroin. Nat. Protoc. *6*, 1612–1631. https://doi.org/10.1038/nprot.2011.379.
37. Li, G., and Sun, S. (2022). Silk fibroin-based biomaterials for tissue engineering applications. Molecules *27*, 2757. https://doi.org/10.3390/molecules27092757.
38. Jian, M., Zhang, Y., and Liu, Z. (2020). Natural biopolymers for flexible sensing and energy devices. Chin. J. Polym. Sci. *38*, 459–490. https://doi.org/10.1007/s10118-020-2379-9.
39. Wu, R., Ma, L., and Liu, X.Y. (2022). From mesoscopic functionalization of silk fibroin to smart fiber devices for textile electronics and photonics. Adv. Sci. *9*, 2103981. https://doi.org/10.1002/advs.202103981.
40. Lu, L., Fan, W., Ge, S., Liew, R.K., Shi, Y., Dou, H., Wang, S., and Lam, S.S. (2022). Progress in recycling and valorization of

waste silk. Sci. Total Environ. *830*, 154812. https://doi.org/10.1016/j.scitotenv.2022.154812.

41. Zhang, C., Zhang, Y., Shao, H., and Hu, X. (2016). Hybrid silk fibers dry-spun from regenerated silk fibroin/graphene oxide aqueous solutions. ACS Appl. Mater. Interfaces *8*, 3349–3358. https://doi.org/10.1021/acsami.5b11245.
42. Liang, X., Li, H., Dou, J., Wang, Q., He, W., Wang, C., Li, D., Lin, J.M., and Zhang, Y. (2020). Stable and biocompatible carbon nanotube ink mediated by silk protein for printed electronics. Adv. Mater. *32*, 2000165. https://doi.org/10.1002/adma.202000165.
43. Chao, M., He, L., Gong, M., Li, N., Li, X., Peng, L., Shi, F., Zhang, L., and Wan, P. (2021). Breathable $Ti_3C_2T_x$ MXene/protein nanocomposites for ultrasensitive medical pressure sensor with degradability in solvents. ACS Nano *15*, 9746–9758. https://doi.org/10.1021/acsnano.1c00472.
44. Lu, Q., Wang, X., Zhu, H., and Kaplan, D.L. (2011). Surface immobilization of antibody on silk fibroin through conformational transition. Acta. Biomater *7*, 2782–2786. https://doi.org/10.1016/j.actbio.2011.03.001.
45. Chen, X., Shao, Z., Knight, D.P., and Vollrath, F. (2007). Conformation transition kinetics of *Bombyx mori* silk protein. Proteins *68*, 223–231. https://doi.org/10.1002/prot.21414.
46. Cheng, Y., Koh, L.D., Li, D., Ji, B., Han, M.Y., and Zhang, Y.W. (2014). On the strength of β-sheet crystallites of *Bombyx mori* silk fibroin. J. R. Soc. Interface *11*, 20140305. https://doi.org/10.1098/rsif.2014.0305.
47. Jin, H.J., Park, J., Karageorgiou, V., Kim, U.J., Valluzzi, R., Cebe, P., and Kaplan, D.L. (2005). Water stable silk films with reduced β sheet content. Adv. Funct. Mater. *15*, 1241–1247. https://doi.org/10.1002/adfm.200400405.
48. Hu, X., Shmelev, K., Sun, L., Gil, E.S., Park, S.H., Cebe, P., and Kaplan, D.L. (2011). Regulation of silk material structure by temperature-controlled water vapor annealing. Biomacromolecules *12*, 1686–1696. https://doi.org/10.1021/bm200062a.
49. Qi, C., Liu, J., Jin, Y., Xu, L., Wang, G., Wang, Z., and Wang, L. (2018). Photo-crosslinkable, injectable sericin hydrogel as 3D biomimetic extracellular matrix for minimally invasive repairing cartilage. Biomaterials *163*, 89–104. https://doi.org/10.1016/j.biomaterials.2018.02.016.
50. Jena, K., Pandey, J.P., Kumari, R., Sinha, A.K., Gupta, V.P., and Singh, G.P. (2018). Free radical scavenging potential of sericin obtained from various ecoraces of tasar cocoons and its cosmeceuticals implication. Int. J. Biol. Macromol. *120*, 255–262. https://doi.org/10.1016/j.ijbiomac.2018.08.090.
51. Liu, J., Shi, L., Deng, Y., Zou, M., Cai, B., Song, Y., Wang, Z., and Wang, L. (2022). Silk sericin-based materials for biomedical applications. Biomaterials *287*, 121638. https://doi.org/10.1016/j.biomaterials.2022.121638.
52. Cao, T.T., and Zhang, Y.Q. (2016). Processing and characterization of silk sericin from *Bombyx mori* and its application in biomaterials and biomedicines. Mater. Sci. Eng. C. *61*, 940–952. https://doi.org/10.1016/j.msec.2015.12.082.
53. Wang, Y.J., and Zhag, Y.Q. (2011). Three-layered Sericins Around the Silk Fibroin Fiber from *Bombyx mori* Cocoon and Their Amino Acid Composition (Trans Tech Publ), pp. 158–163.
54. Wang, Z., Zhang, Y., Zhang, J., Huang, L., Liu, J., Li, Y., Zhang, G., Kundu, S.C., and Wang, L. (2014). Exploring natural silk protein sericin for regenerative medicine: an injectable, photoluminescent, cell-adhesive 3D hydrogel. Sci. Rep. *4*, 7064. https://doi.org/10.1038/srep07064.
55. Dash, R., Mukherjee, S., and Kundu, S.C. (2006). Isolation, purification and characterization of silk protein sericin from cocoon peduncles of tropical tasar silkworm. Int. J. Biol. Macromol. *38*, 255–258. https://doi.org/10.1016/j.ijbiomac.2006.03.001.
56. Teramoto, H., Kakazu, A., Yamauchi, K., and Asakura, T. (2007). Role of hydroxyl side chains in *Bombyx mori* silk sericin in stabilizing its solid structure. Macromolecules *40*, 1562–1569. https://doi.org/10.1021/ma062604e.
57. Liu, H., Qin, S., Liu, J., Zhou, C., Zhu, Y., Yuan, Y., Fu, D., Lv, Q., Song, Y., Zou, M., et al. (2022). Bio-inspired self-hydrophobized sericin adhesive with tough underwater adhesion enables wound healing and fluid leakage sealing. Adv. Funct. Mater. *32*, 2201108. https://doi.org/10.1002/adfm.202201108.
58. Zhang, Y.Q. (2002). Applications of natural silk protein sericin in biomaterials. Biotechnol. Adv. *20*, 91–100. https://doi.org/10.1016/s0734-9750(02)00003-4.
59. Mario Cheong, G.L., Lim, K.S., Jakubowicz, A., Martens, P.J., Poole-Warren, L.A., and Green, R.A. (2014). Conductive hydrogels with tailored bioactivity for implantable electrode coatings. Acta. Biomater *10*, 1216–1226. https://doi.org/10.1016/j.actbio.2013.12.032.
60. Li, J., Wang, B.-X., Cheng, D.-H., Liu, Z.-M., Lv, L.-H., Guo, J., and Lu, Y.-H. (2021). Electrospun sericin/PNIPAM-based nano-modified cotton fabric with multi-function responsiveness. Coatings *11*, 632. https://doi.org/10.3390/coatings11060632.
61. Chen, S., Xie, J., Liu, J., Huang, X., and Wang, C. (2021). Transparent, highly-stretchable, adhesive, and ionic conductive composite hydrogel for biomimetic skin. J. Mater. Sci. *56*, 2725–2737. https://doi.org/10.1007/s10853-020-05382-z.
62. Duan, Q., and Lu, Y. (2021). Silk sericin as a green adhesive to fabricate a textile strain sensor with excellent electromagnetic shielding performance. ACS Appl. Mater. Interfaces *13*, 28832–28842. https://doi.org/10.1021/acsami.1c05671.
63. Ma, H., Li, J., Zhou, J., Luo, Q., Wu, W., Mao, Z., and Ma, W. (2022). Screen-printed carbon black/recycled sericin@fabrics for wearable sensors to monitor sweat loss. ACS Appl. Mater. Interfaces *14*, 11813–11819. https://doi.org/10.1021/acsami.1c23341.
64. Hu, Z., Shao, Q., Xu, X., Zhang, D., and Huang, Y. (2017). Surface initiated grafting of polymer chains on carbon nanotubes via one-step cycloaddition of diarylcarbene. Compos. Sci. Technol. *142*, 294–301. https://doi.org/10.1016/j.compscitech.2017.02.027.
65. Rider, A., Yeo, E., Gopalakrishna, J., Thostenson, E., and Brack, N. (2015). Hierarchical composites with high-volume fractions of carbon nanotubes: Influence of plasma surface treatment and thermoplastic nanophase-modified epoxy. Carbon *94*, 971–981. https://doi.org/10.1016/j.carbon.2015.07.076.
66. Preston, C., Song, D., Dai, J., Tsinas, Z., Bavier, J., Cumings, J., Ballarotto, V., and Hu, L. (2015). Scalable nanomanufacturing of surfactant-free carbon nanotube inks for spray coatings with high conductivity. Nano Res. *8*, 2242–2250. https://doi.org/10.1007/s12274-015-0735-9.
67. Zhao, L., Wen, Z., Jiang, F., Zheng, Z., and Lu, S. (2020). Silk/polyols/GOD microneedle based electrochemical biosensor for continuous glucose monitoring. RSC Adv. *10*, 6163–6171. https://doi.org/10.1039/c9ra10374k.
68. Chu, T., Wang, H., Qiu, Y., Luo, H., He, B., Wu, B., and Gao, B. (2021). 3D printed smart silk wearable sensors. Analyst *146*, 1552–1558. https://doi.org/10.1039/d0an02292f.
69. Choudhary, T., Rajamanickam, G.P., and Dendukuri, D. (2015). Woven electrochemical fabric-based test sensors (WEFTS): a new class of multiplexed electrochemical sensors. Lab Chip *15*, 2064–2072. https://doi.org/10.1039/c5lc00041f.
70. Liu, X., Zhang, W., Lin, Z., Meng, Z., Shi, C., Xu, Z., Yang, L., and Liu, X.Y. (2021). Coupling of silk fibroin nanofibrils enzymatic membrane with ultra-thin PtNPs/graphene film to acquire long and stable on-skin sweat glucose and lactate sensing. Small Methods *5*, 2000926. https://doi.org/10.1002/smtd.202000926.
71. Meng, G., Long, F., Zeng, Z., Kong, L., Zhao, B., Yan, J., Yang, L., Yang, Y., Liu, X.Y., Yan, Z., and Lin, N. (2023). Silk fibroin based wearable electrochemical sensors with biomimetic enzyme-like activity constructed for durable and on-site health monitoring. Biosens. Bioelectron. *228*, 115198. https://doi.org/10.1016/j.bios.2023.115198.
72. Promphet, N., Phamonpon, W., Karintrithip, W., Rattanawaleedirojn, P., Saengkiettiyut, K., Boonyongmaneerat, Y., and Rodthongkum, N. (2023). Carbonization of self-reduced AuNPs on silk as wearable skin patches for non-invasive sweat urea detection. Int. J. Biol. Macromol. *242*, 124757. https://doi.org/10.1016/j.ijbiomac.2023.124757.
73. Liang, B., Fang, L., Hu, Y., Yang, G., Zhu, Q., and Ye, X. (2014). Fabrication and application of flexible graphene silk composite film electrodes decorated with spiky Pt nanospheres. Nanoscale *6*, 4264–4274. https://doi.org/10.1039/c3nr06057h.
74. Liu, J., Yang, M., Tan, J., Yin, Y., Yang, Y., and Wang, C. (2022). pH-responsive discoloration silk fibroin films based on prodigiosin from microbial fermentation. Dyes Pigm. *198*, 109994. https://doi.org/10.1016/j.dyepig.2021.109994.
75. Xiao, G., He, J., Qiao, Y., Wang, F., Xia, Q., Wang, X., Yu, L., Lu, Z., and Li, C.-M. (2020). Facile and low-cost fabrication of a thread/paper-based wearable system for simultaneous detection of lactate and pH in human sweat. Adv. Fiber Mater. *2*, 265–278. https://doi.org/10.1007/s42765-020-00046-8.
76. Zhang, Y., Liao, J., Li, Z., Hu, M., Bian, C., and Lin, S. (2023). All fabric and flexible wearable sensors for simultaneous sweat metabolite detection and high-efficiency collection. Talanta *260*, 124610. https://doi.org/10.1016/j.talanta.2023.124610.

77. Gogurla, N., Kim, Y., Cho, S., Kim, J., and Kim, S. (2021). Multifunctional and ultrathin electronic tattoo for on-skin diagnostic and therapeutic applications. Adv. Mater. *33*, 2008308. https://doi.org/10.1002/adma.202008308.
78. Wu, R., Ma, L., Hou, C., Meng, Z., Guo, W., Yu, W., Yu, R., Hu, F., and Liu, X.Y. (2019). Silk composite electronic textile sensor for high space precision 2D combo temperature-pressure sensing. Small *15*, 1901558. https://doi.org/10.1002/smll.201901558.
79. Duan, S., Shi, Q., Hong, J., Zhu, D., Lin, Y., Li, Y., Lei, W., Lee, C., and Wu, J. (2023). Water-modulated biomimetic hyper-attribute-gel electronic skin for robotics and skin-attachable wearables. ACS Nano *17*, 1355–1371. https://doi.org/10.1021/acsnano.2c09851.
80. Wang, C., Xia, K., Zhang, M., Jian, M., and Zhang, Y. (2017). An all-silk-derived dual-mode E-skin for simultaneous temperature-pressure detection. ACS Appl. Mater. Interfaces *9*, 39484–39492. https://doi.org/10.1021/acsami.7b13356.
81. Cho, H., Lee, C., Lee, C., Lee, S., and Kim, S. (2023). Robust, ultrathin, and highly sensitive reduced graphene oxide/silk fibroin wearable sensors responded to temperature and humidity for physiological detection. Biomacromolecules *24*, 2606–2617. https://doi.org/10.1021/acs.biomac.3c00106.
82. Wang, C., Zhu, M., Yu, H.Y., Abdalkarim, S.Y.H., Ouyang, Z., Zhu, J., and Yao, J. (2021). Multifunctional biosensors made with self-healable silk fibroin imitating skin. ACS Appl. Mater. Interfaces *13*, 33371–33382. https://doi.org/10.1021/acsami.1c08568.
83. Zheng, W., Cai, X., Yan, D., Murtaza, G., Meng, Z., and Qiu, L. (2022). Dual-responsive photonic crystal sensors based on physical crossing-linking SF-PNIPAM dual-crosslinked hydrogel. Gels *8*, 339. https://doi.org/10.3390/gels8060339.
84. Wang, Y., Ren, J., Ye, C., Pei, Y., and Ling, S. (2021). Thermochromic silks for temperature management and dynamic textile displays. Nano-Micro Lett. *13*, 72. https://doi.org/10.1007/s40820-021-00591-w.
85. Chen, G., Matsuhisa, N., Liu, Z., Qi, D., Cai, P., Jiang, Y., Wan, C., Cui, Y., Leow, W.R., Liu, Z., et al. (2018). Plasticizing silk protein for on-skin stretchable electrodes. Adv. Mater. *30*, 1800129. https://doi.org/10.1002/adma.201800129.
86. Li, Q., Chen, G., Cui, Y., Ji, S., Liu, Z., Wan, C., Liu, Y., Lu, Y., Wang, C., Zhang, N., et al. (2021). Highly thermal-wet comfortable and conformal silk-based electrodes for on-skin sensors with sweat tolerance. ACS Nano *15*, 9955–9966. https://doi.org/10.1021/acsnano.1c01431.
87. Zhao, J., Deng, J., Liang, W., Zhao, L., Dong, Y., Wang, X., and Lin, L. (2022). Water-retentive, 3D knitted textile electrode for long-term and motion state bioelectrical signal acquisition. Compos. Sci. Technol. *227*, 109606. https://doi.org/10.1016/j.compscitech.2022.109606.
88. Wang, D., Wang, L., Lou, Z., Zheng, Y., Wang, K., Zhao, L., Han, W., Jiang, K., and Shen, G. (2020). Biomimetic, biocompatible and robust silk fibroin-MXene film with stable 3D cross-link structure for flexible pressure sensors. Nano Energy *78*, 105252. https://doi.org/10.1016/j.nanoen.2020.105252.
89. He, Y., Zhou, M., Mahmoud, M.H.H., Lu, X., He, G., Zhang, L., Huang, M., Elnaggar, A.Y., Lei, Q., Liu, H., et al. (2022). Multifunctional wearable strain/pressure sensor based on conductive carbon nanotubes/silk nonwoven fabric with high durability and low detection limit. Adv. Compos. Hybrid Mater. *5*, 1939–1950. https://doi.org/10.1007/s42114-022-00525-z.
90. Mao, C., Zhang, H., and Lu, Z. (2017). Flexible and wearable electronic silk fabrics for human physiological monitoring. Smart Mater. Struct. *26*, 095033. https://doi.org/10.1088/1361-665X/aa782d.
91. Bi, S., Hai, W., Wang, L., Xu, K., Chen, Q., Chen, C., Yu, Q., Chen, C., Li, M., Shao, H., et al. (2023). Green one-step strategy of conductive ink for active health monitoring in rehabilitation and early care. ACS Appl. Mater. Interfaces *15*, 57593–57601. https://doi.org/10.1021/acsami.3c12851.
92. Xing, L., Wang, Y., Cheng, J., Chen, G., and Xing, T. (2023). Robust and flexible smart silk/PEDOT conductive fibers as wearable sensor for personal health management and information transmission. Int. J. Biol. Macromol. *248*, 125870. https://doi.org/10.1016/j.ijbiomac.2023.125870.
93. Wang, C., Li, X., Gao, E., Jian, M., Xia, K., Wang, Q., Xu, Z., Ren, T., and Zhang, Y. (2016). Carbonized silk fabric for ultrastretchable, highly sensitive, and wearable strain sensors. Adv. Mater. *28*, 6640–6648. https://doi.org/10.1002/adma.201601572.
94. Wang, C., Xia, K., Jian, M., Wang, H., Zhang, M., and Zhang, Y. (2017). Carbonized silk georgette as an ultrasensitive wearable strain sensor for full-range human activity monitoring. J. Mater. Chem. C *5*, 7604–7611. https://doi.org/10.1039/C7TC01962A.
95. Dong, Y., Xu, D., Yu, H.-Y., Mi, Q., Zou, F., and Yao, X. (2023). Highly sensitive, scrub-resistant, robust breathable wearable silk yarn sensors via interfacial multiple covalent reactions for health management. Nano Energy *115*, 108723. https://doi.org/10.1016/j.nanoen.2023.108723.
96. Cai, H., Liu, Z., Xu, M., Chen, L., Chen, X., Cheng, L., Li, Z., and Dai, F. (2021). High performance flexible silk fabric electrodes with antibacterial, flame retardant and UV resistance for supercapacitors and sensors. Electrochim. Acta *390*, 138895. https://doi.org/10.1016/j.electacta.2021.138895.
97. Ouyang, Z., Li, S., Liu, J., Yu, H.-Y., Peng, L., Zheng, S., Xu, D., and Tam, K.C. (2022). Bottom-up reconstruction of smart textiles with hierarchical structures to assemble versatile wearable devices for multiple signals monitoring. Nano Energy *104*, 107963. https://doi.org/10.1016/j.nanoen.2022.107963.
98. Jiang, Y., Ma, J., Shen, L., Zhang, W., Yang, K., Zhu, B., Yang, Y., Ma, H., Chen, X., Bai, S., and Zhu, N. (2023). Chemresistor smart sensors from silk fibroin-graphene composites for touch-free wearables. ACS Appl. Mater. Interfaces *15*, 47196–47207. https://doi.org/10.1021/acsami.3c07913.
99. Ma, L., Liu, Q., Wu, R., Meng, Z., Patil, A., Yu, R., Yang, Y., Zhu, S., Fan, X., Hou, C., et al. (2020). From molecular reconstruction of mesoscopic functional conductive silk fibrous materials to remote respiration monitoring. Small *16*, 2000203. https://doi.org/10.1002/smll.202000203.
100. Zhao, L., Zhao, J., Zhang, F., Xu, Z., Chen, F., Shi, Y., Hou, C., Huang, Y., Lin, C., Yu, R., and Guo, W. (2021). Highly stretchable, adhesive, and self-healing silk fibroin-dopted hydrogels for wearable sensors. Adv. Healthc. Mater. *10*, 2002083. https://doi.org/10.1002/adhm.202002083.
101. Wen, D.-L., Pang, Y.-X., Huang, P., Wang, Y.-L., Zhang, X.-R., Deng, H.-T., and Zhang, X.-S. (2022). Silk fibroin-based wearable all-fiber multifunctional sensor for smart clothing. Adv. Fiber Mater. *4*, 873–884. https://doi.org/10.1007/s42765-022-00150-x.
102. Yue, L., Gong, M., Wang, J., Ma, S., Chen, Q., Kong, X., Lin, X., Zhang, L., Wu, Z., and Wang, D. (2023). Hygroscopic MXene/protein nanocomposite fibers enabling highly stretchable, antifreezing, repairable, and degradable skin-like wearable electronics. ACS Mater. Lett. *5*, 2104–2113. https://doi.org/10.1021/acsmaterialslett.3c00397.
103. Zheng, H., Lin, N., He, Y., and Zuo, B. (2021). Self-healing, self-adhesive silk fibroin conductive hydrogel as a flexible strain sensor. ACS Appl. Mater. Interfaces *13*, 40013–40031. https://doi.org/10.1021/acsami.1c08395.
104. Wang, T., Lu, J., Shi, L., Chen, G., Xu, M., Xu, Y., Su, Q., Mu, Y., Chen, L., Hu, R., et al. (2020). Association of insulin resistance and β-cell dysfunction with incident diabetes among adults in China: a nationwide, population-based, prospective cohort study. Lancet Diabetes Endo *8*, 115–124. https://doi.org/10.1016/s2213-8587(19)30425-5.
105. Wang, L., Gao, P., Zhang, M., Huang, Z., Zhang, D., Deng, Q., Li, Y., Zhao, Z., Qin, X., Jin, D., et al. (2017). Prevalence and ethnic pattern of diabetes and prediabetes in China in 2013. JAMA *317*, 2515–2523. https://doi.org/10.1001/jama.2017.7596.
106. Lee, H., Hong, Y.J., Baik, S., Hyeon, T., and Kim, D.H. (2018). Enzyme-based glucose sensor: from invasive to wearable device. Adv. Healthc. Mater. *7*, 1701150. https://doi.org/10.1002/adhm.201701150.
107. Saha, T., Del Caño, R., Mahato, K., De la Paz, E., Chen, C., Ding, S., Yin, L., and Wang, J. (2023). Wearable electrochemical glucose sensors in diabetes management: a comprehensive review. Chem. Rev. *123*, 7854–7889. https://doi.org/10.1021/acs.chemrev.3c00078.
108. Lu, S., Wang, X., Lu, Q., Hu, X., Uppal, N., Omenetto, F.G., and Kaplan, D.L. (2009). Stabilization of enzymes in silk films. Biomacromolecules *10*, 1032–1042. https://doi.org/10.1021/bm800956n.
109. Huang, Y., Ren, J., and Qu, X. (2019). Nanozymes: classification, catalytic mechanisms, activity regulation, and applications. Chem. Rev. *119*, 4357–4412. https://doi.org/10.1021/acs.chemrev.8b00672.
110. Hafez, M.E., Ma, H., Ma, W., and Long, Y.T. (2019). Unveiling the intrinsic catalytic activities of single-gold-nanoparticle-based enzyme mimetics. Angew. Chem. Int. Ed. *58*, 6327–6332. https://doi.org/10.1002/anie.201901384.
111. Huang, L., Li, C., Yuan, W., and Shi, G. (2013). Strong composite films with layered structures prepared by casting silk fibroin-graphene oxide hydrogels. Nanoscale *5*, 3780–3786. https://doi.org/10.1039/c3nr00196b.
112. Hu, K., Gupta, M.K., Kulkarni, D.D., and Tsukruk, V.V. (2013). Ultra-robust graphene

oxide-silk fibroin nanocomposite membranes. Adv. Mater. *25*, 2301–2307. https://doi.org/10.1002/adma.201300179.

113. Shi, J., Zhang, H., Snyder, A., Wang, M.X., Xie, J., Marshall Porterfield, D., and Stanciu, L.A. (2012). An aqueous media based approach for the preparation of a biosensor platform composed of graphene oxide and Pt-black. Biosens. Bioelectron. *38*, 314–320. https://doi.org/10.1016/j.bios.2012.06.007.
114. Zeng, G., Xing, Y., Gao, J., Wang, Z., and Zhang, X. (2010). Unconventional layer-by-layer assembly of graphene multilayer films for enzyme-based glucose and maltose biosensing. Langmuir *26*, 15022–15026. https://doi.org/10.1021/la102806v.
115. Cao, X., Ye, Y., Li, Y., Xu, X., Yu, J., and Liu, S. (2013). Self-assembled glucose oxidase/graphene/gold ternary nanocomposites for direct electrochemistry and electrocatalysis. J. Electroanal. Chem. *697*, 10–14. https://doi.org/10.1016/j.jelechem.2013.03.001.
116. Gong, J., Ren, Y., Fu, R., Li, Z., and Zhang, J. (2017). pH-mediated antibacterial dyeing of cotton with prodigiosins nanomicelles produced by microbial fermentation. Polymers *9*, 468. https://doi.org/10.3390/polym9100468.
117. Koh, L.D., Yeo, J., Lee, Y.Y., Ong, Q., Han, M., and Tee, B.C.K. (2018). Advancing the frontiers of silk fibroin protein-based materials for futuristic electronics and clinical wound-healing (Invited review). Mater. Sci. Eng. C *86*, 151–172. https://doi.org/10.1016/j.msec.2018.01.007.
118. Samak, N.A., Selim, M.S., Hao, Z., and Xing, J. (2022). Immobilized arginine/tryptophan-rich cyclic dodecapeptide on reduced graphene oxide anchored with manganese dioxide for microbial biofilm eradication. J. Hazard Mater. *426*, 128035. https://doi.org/10.1016/j.jhazmat.2021.128035.
119. Zhu, J., Andres, C.M., Xu, J., Ramamoorthy, A., Tsotsis, T., and Kotov, N.A. (2012). Pseudonegative thermal expansion and the state of water in graphene oxide layered assemblies. ACS Nano *6*, 8357–8365. https://doi.org/10.1021/nn3031244.
120. Moraes, M.R., Alves, A.C., Toptan, F., Martins, M.S., Vieira, E.M.F., Paleo, A.J., Souto, A.P., Santos, W.L.F., Esteves, M.F., and Zille, A. (2017). Glycerol/PEDOT: PSS coated woven fabric as a flexible heating element on textiles. J. Mater. Chem. C *5*, 3807–3822. https://doi.org/10.1039/C7TC00486A.
121. Wu, X., Wang, Z., Yu, M., Xiu, L., and Qiu, J. (2017). Stabilizing the MXenes by carbon nanoplating for developing hierarchical nanohybrids with efficient lithium storage and hydrogen evolution capability. Adv. Mater. *29*, 1607017. https://doi.org/10.1002/adma.201607017.
122. Bae, J.H., and Jeon, Y.J. (2021). Pulse sharpness as a quantitative index of vascular aging. Sci. Rep. *11*, 19895. https://doi.org/10.1038/s41598-021-99315-8.
123. Ke, X., Dong, Z., Tang, S., Chu, W., Zheng, X., Zhen, L., Chen, X., Ding, C., Luo, J., and Li, J. (2020). A natural polymer based bioadhesive with self-healing behavior and improved antibacterial properties. Biomater. Sci. *8*, 4346–4357. https://doi.org/10.1039/d0bm00624f.
124. Yang, Y., Song, X., Li, X., Chen, Z., Zhou, C., Zhou, Q., and Chen, Y. (2018). Recent progress in biomimetic additive manufacturing technology: from materials to functional structures. Adv. Mater. *30*, 1706539. https://doi.org/10.1002/adma.201706539.
125. Gong, S., Yap, L.W., Zhu, B., and Cheng, W. (2020). Multiscale soft–hard interface design for flexible hybrid electronics. Adv. Mater. *32*, 1902278. https://doi.org/10.1002/adma.201902278.
126. Liu, X., Liu, J., Wang, J., Wang, T., Jiang, Y., Hu, J., Liu, Z., Chen, X., and Yu, J. (2020). Bioinspired, microstructured silk fibroin adhesives for flexible skin sensors. ACS Appl. Mater. Interfaces *12*, 5601–5609. https://doi.org/10.1021/acsami.9b21197.
127. Baik, S., Kim, D.W., Park, Y., Lee, T.J., Ho Bhang, S., and Pang, C. (2017). A wet-tolerant adhesive patch inspired by protuberances in suction cups of octopi. Nature *546*, 396–400. https://doi.org/10.1038/nature22382.
128. O'Connor, R.J., Ogle, J., and Odio, M. (2016). Induction of epidermal damage by tape stripping to evaluate skin mildness of cleansing regimens for the premature epidermal barrier. Int. J. Dermatol. *55*, 21–27. https://doi.org/10.1111/ijd.13373.
129. Yuk, H., Zhang, T., Lin, S., Parada, G.A., and Zhao, X. (2016). Tough bonding of hydrogels to diverse non-porous surfaces. Nat. Mater. *15*, 190–196. https://doi.org/10.1038/nmat4463.
130. Xu, L., Huang, Z., Deng, Z., Du, Z., Sun, T.L., Guo, Z.H., and Yue, K. (2021). A transparent, highly stretchable, solvent-resistant, recyclable multifunctional ionogel with underwater self-healing and adhesion for reliable strain sensors. Adv. Mater. *33*, 2105306. https://doi.org/10.1002/adma.202105306.
131. Yu, Z., and Wu, P. (2021). Underwater communication and optical camouflage ionogels. Adv. Mater. *33*, 2008479. https://doi.org/10.1002/adma.202008479.
132. Rose, S., Prevoteau, A., Elzière, P., Hourdet, D., Marcellan, A., and Leibler, L. (2014). Nanoparticle solutions as adhesives for gels and biological tissues. Nature *505*, 382–385. https://doi.org/10.1038/nature12806.
133. Lee, S., Inoue, Y., Kim, D., Reuveny, A., Kuribara, K., Yokota, T., Reeder, J., Sekino, M., Sekitani, T., Abe, Y., and Someya, T. (2014). A strain-absorbing design for tissue-machine interfaces using a tunable adhesive gel. Nat. Commun. *5*, 5898. https://doi.org/10.1038/ncomms6898.
134. Jeong, S.H., Zhang, S., Hjort, K., Hilborn, J., and Wu, Z. (2016). PDMS-based elastomer tuned soft, stretchable, and sticky for epidermal electronics. Adv. Mater. *28*, 5830–5836. https://doi.org/10.1002/adma.201505372.
135. Johnston, E.R., Miyagi, Y., Chuah, J.-A., Numata, K., and Serban, M.A. (2018). Interplay between silk fibroin's structure and its adhesive properties. ACS Biomater. Sci. Eng. *4*, 2815–2824. https://doi.org/10.1021/acsbiomaterials.8b00544.
136. Gao, X., Dai, Q., Yao, L., Dong, H., Li, Q., and Cao, X. (2020). A medical adhesive used in a wet environment by blending tannic acid and silk fibroin. Biomater. Sci. *8*, 2694–2701. https://doi.org/10.1039/d0bm00322k.
137. Tutar, R., Yüce-Erarslan, E., İzbudak, B., and Bal-Öztürk, A. (2022). Photocurable silk fibroin-based tissue sealants with enhanced adhesive properties for the treatment of corneal perforations. J. Mater. Chem. B *10*, 2912–2925. https://doi.org/10.1039/d1tb02502c.
138. Seo, J.W., Kim, H., Kim, K., Choi, S.Q., and Lee, H.J. (2018). Calcium-modified silk as a biocompatible and strong adhesive for epidermal electronics. Adv. Funct. Mater. *28*, 1800802. https://doi.org/10.1002/adfm.201800802.
139. Lee, S.M., Lee, T., Kim, H., Jo, Y., Kim, M.G., Kim, S., Bae, H.M., and Lee, H.J. (2021). Calcium-modified silk patch as a next-generation ultrasound coupling medium. ACS Appl. Mater. Interfaces *13*, 55827–55839. https://doi.org/10.1021/acsami.1c16735.
140. Wang, J., Zhang, N., Tan, Y., Fu, F., Liu, G., Fang, Y., Zhang, X.X., Liu, M., Cheng, Y., and Yu, J. (2022). Sweat-resistant silk fibroin-based double network hydrogel adhesives. ACS Appl. Mater. Interfaces *14*, 21945–21953. https://doi.org/10.1021/acsami.2c02534.
141. Chen, Y.C., and Chen, Y.H. (2019). Thermo and pH-responsive methylcellulose and hydroxypropyl methylcellulose hydrogels containing K_2SO_4 for water retention and a controlled-release water-soluble fertilizer. Sci. Total Environ. *655*, 958–967. https://doi.org/10.1016/j.scitotenv.2018.11.264.
142. Sun, L., Zhou, Z., Zhong, J., Shi, Z., Mao, Y., Li, H., Cao, J., and Tao, T.H. (2020). Implantable, degradable, therapeutic terahertz metamaterial devices. Small *16*, 2000294. https://doi.org/10.1002/smll.202000294.
143. Carrero, J.J., Hecking, M., Ulasi, I., Sola, L., and Thomas, B. (2017). Chronic kidney disease, gender, and access to care: a global perspective. Semin. Nephrol. *37*, 296–308. https://doi.org/10.1016/j.semnephrol.2017.02.009.
144. Yang, N., Qi, P., Ren, J., Yu, H., Liu, S., Li, J., Chen, W., Kaplan, D.L., and Ling, S. (2019). Polyvinyl alcohol/silk fibroin/borax hydrogel ionotronics: a highly stretchable, self-healable, and biocompatible sensing platform. ACS Appl. Mater. Interfaces *11*, 23632–23638. https://doi.org/10.1021/acsami.9b06920.
145. Sultan, M.T., Moon, B.M., Yang, J.W., Lee, O.J., Kim, S.H., Lee, J.S., Lee, Y.J., Seo, Y.B., Kim, D.Y., Ajiteru, O., et al. (2019). Recirculating peritoneal dialysis system using urease-fixed silk fibroin membrane filter with spherical carbonaceous adsorbent. Mater. Sci. Eng. C. *97*, 55–66. https://doi.org/10.1016/j.msec.2018.12.021.
146. Moon, B.M., Choi, M.J., Sultan, M.T., Yang, J.W., Ju, H.W., Lee, J.M., Park, H.J., Park, Y.R., Kim, S.H., Kim, D.W., et al. (2017). Novel fabrication method of the peritoneal dialysis filter using silk fibroin with urease fixation system. J. Biomed. Mater. Res. B Appl. Biomater. *105*, 2136–2144. https://doi.org/10.1002/jbm.b.33751.
147. Tan, X., Wang, Y., Du, W., and Mu, T. (2020). Top-down extraction of silk protein nanofibers by natural deep eutectic solvents and application in dispersion of multiwalled carbon nanotubes for wearable sensing. ChemSusChem *13*, 321–327. https://doi.org/10.1002/cssc.201902979.
148. Wang, C., Yokota, T., and Someya, T. (2021). Natural biopolymer-based biocompatible conductors for stretchable bioelectronics. Chem. Rev. *121*, 2109–2146. https://doi.org/10.1021/acs.chemrev.0c00897.
149. Hui, Z., Zhang, L., Ren, G., Sun, G., Yu, H.D., and Huang, W. (2023). Green flexible electronics: natural materials, fabrication, and applications. Adv. Mater. *35*, 2211202. https://doi.org/10.1002/adma.202211202.
150. Zhang, Y., Zhou, Z., Fan, Z., Zhang, S., Zheng, F., Liu, K., Zhang, Y., Shi, Z., Chen, L.,

Li, X., et al. (2018). Self-powered multifunctional transient bioelectronics. Small *14*, 1802050. https://doi.org/10.1002/smll.201802050.

151. Zhou, Z., Zhang, S., Cao, Y., Marelli, B., Xia, X., and Tao, T.H. (2018). Engineering the future of silk materials through advanced manufacturing. Adv. Mater. *30*, 1706983. https://doi.org/10.1002/adma.201706983.

152. Zhou, Z., Shi, Z., Cai, X., Zhang, S., Corder, S.G., Li, X., Zhang, Y., Zhang, G., Chen, L., Liu, M., et al. (2017). The use of functionalized silk fibroin films as a platform for optical diffraction-based sensing applications. Adv. Mater. *29*, 1605471. https://doi.org/10.1002/adma.201605471.

153. Kojic, N., Pritchard, E.M., Tao, H., Brenckle, M.A., Mondia, J.P., Panilaitis, B., Omenetto, F., and Kaplan, D.L. (2012). Focal infection treatment using laser-mediated heating of injectable silk hydrogels with gold nanoparticles. Adv. Funct. Mater. *22*, 3793–3798. https://doi.org/10.1002/adfm.201200382.

154. Herrera-Rincon, C., Golding, A.S., Moran, K.M., Harrison, C., Martyniuk, C.J., Guay, J.A., Zaltsman, J., Carabello, H., Kaplan, D.L., and Levin, M. (2018). Brief local application of progesterone via a wearable bioreactor induces long-term regenerative response in adult xenopus hindlimb. Cell Rep. *25*, 1593–1609.e7. https://doi.org/10.1016/j.celrep.2018.10.010.

155. Kanner, A.M., and Bicchi, M.M. (2022). Antiseizure medications for adults with epilepsy: a review. JAMA *327*, 1269–1281. https://doi.org/10.1001/jama.2022.3880.

156. Guan, J., Zhu, W., Liu, B., Yang, K., Vollrath, F., and Xu, J. (2017). Comparing the microstructure and mechanical properties of *Bombyx mori* and *Antheraea pernyi* cocoon composites. Acta Biomater. *47*, 60–70. https://doi.org/10.1016/j.actbio.2016.09.042.